Results from Ring-Diagram Analysis

Sushanta Tripathy
National Solar Observatory, Tucson

Content

- What is Ring-Diagram
- Results from
  - Mode Parameters
  - Sub-surface Structure (sound speed)
  - Sub-surface Flows
  - Connection to Space Weather
- Multi-height and Multi-wavelength Analysis
- Summary

Ring-Diagram Technique

- Ring-diagram is a helioseismic tool to study the near-surface layer of the Sun.
- It is the oldest technique and was developed by Frank Hill (NSO) in 1988. It is fairly easy to use
- The method is analogous to global mode analysis but confined to small areas on the Sun's surface
- The modes measured are typically degree (ℓ) ≥150; which mostly have lower turning point at $R_\Theta \geq 0.95$ (35 Mm below the surface)
- Can be constructed using any spatially and temporally resolved set of observations e.g. velocity or intensity

Ring - Diagram Technique

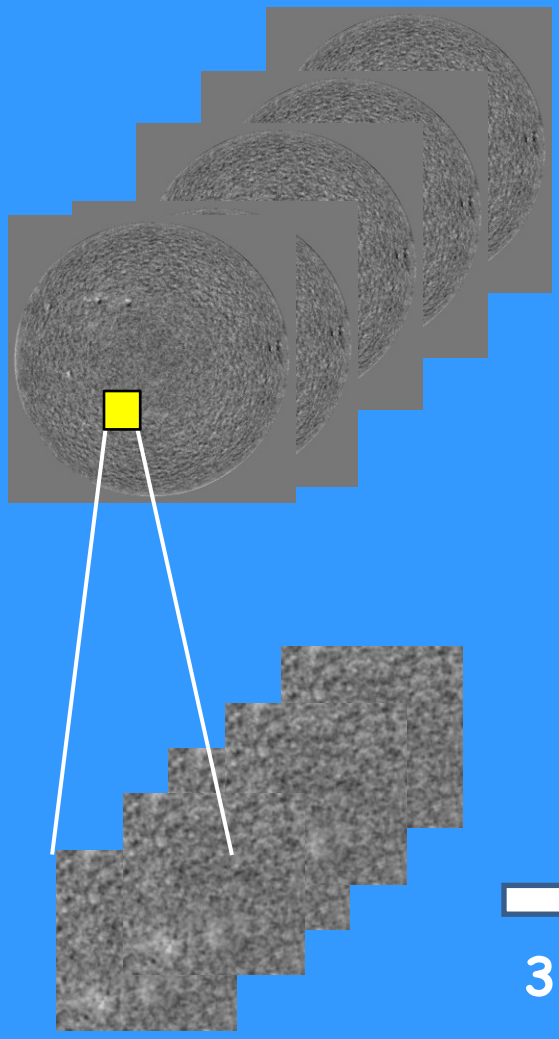

3D-FFT

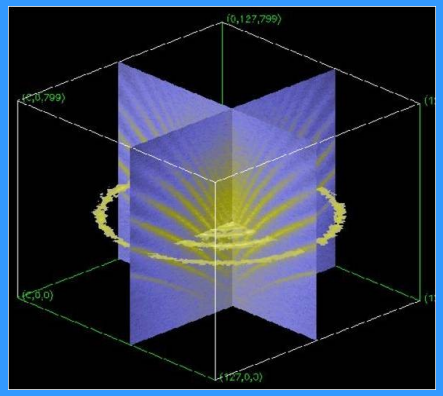

Peak Profile Model

Mode parameters: Frequency, Line width, Amplitude, Background, Velocity (Ux & Uy)

Inversion

Velocity (Vx & Vy) as a function of depth

Ring - Diagram Technique

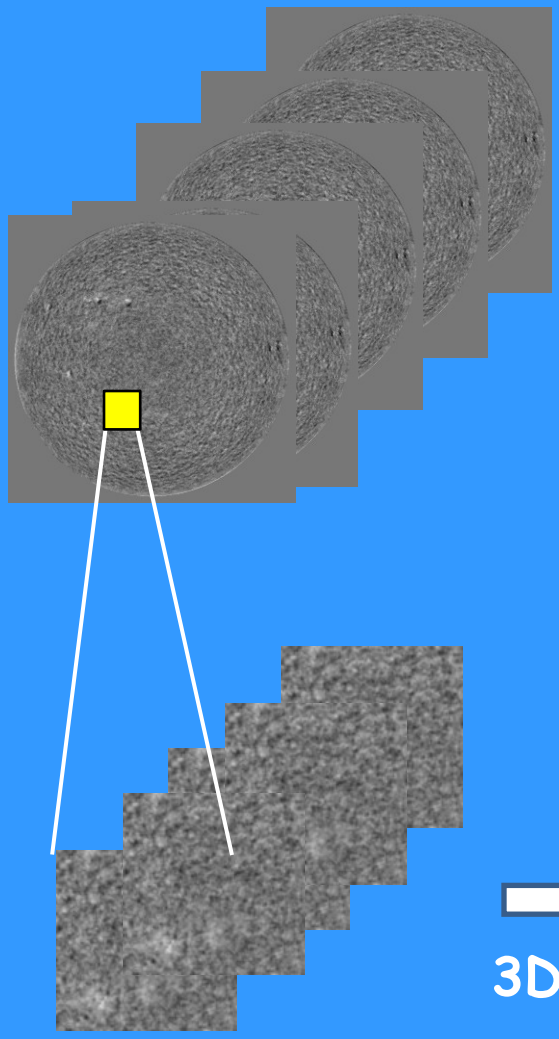

3D-FFT

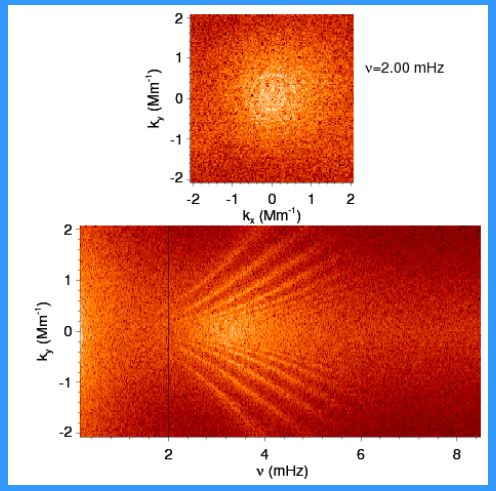

Peak Profile Model

Mode parameters: Frequency, Line width, Amplitude, Background, Velocity (Ux & Uy)

Inversion

Velocity (Vx & Vy) as a function of depth

Power Spectrum

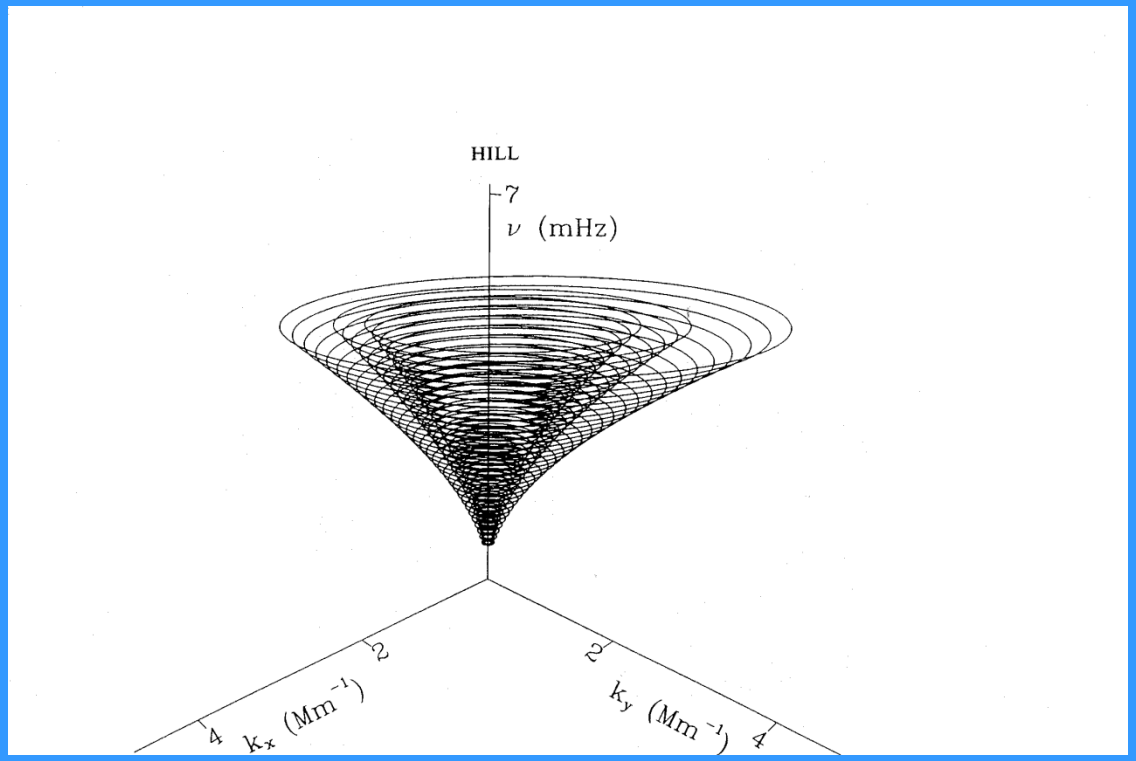

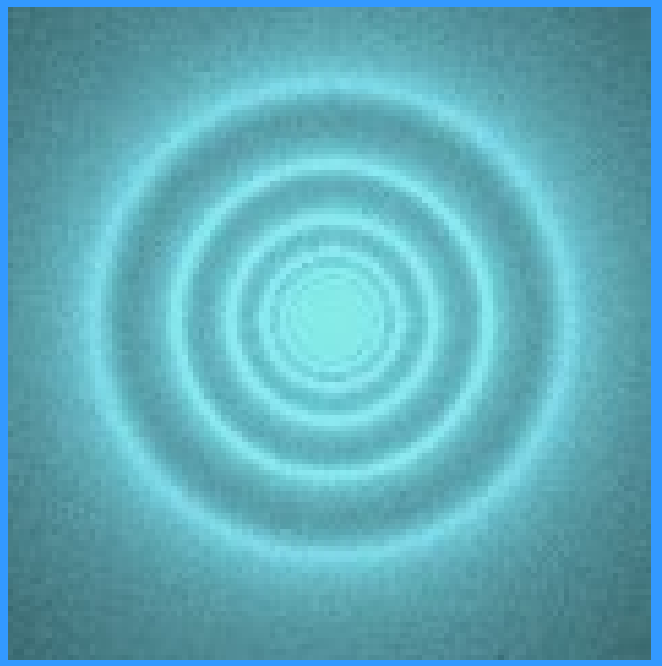

Fitting Technique

- Quantitative analysis of ring-diagrams are undertaken by fitting model spectra profiles to the data.
- Two types of models are normally used: a symmetric Lorentzian and an asymmetric profile:

$$P = \frac{A\Gamma}{(\omega - \omega_0 + k_x U_x + k_y U_y)^2 + \Gamma^2} + \frac{b_0}{k^3}$$

$$P(k_x, k_y, \nu) = \frac{e^{B_1}}{k^3} + \frac{e^{B_2}}{k^4} + \frac{exp(A_0 + (k - k_0)A_1 + A_2(k_x/k)^2 + A_3\frac{k_x k_y}{k^2})S_x}{x^2 + 1}$$

where

$$x = \frac{\nu - ck^p - U_x k_x - U_y k_y}{w_o + w_1(k - k_0)}$$

$$S_x = S^2 + (1 + Sx)^2$$

Fitting Technique

- The fits are obtained using a maximum likelihood function *L* or minimizing the function *F*:

$$F = -\ln L = \sum_i (\ln M_i + \frac{O_i}{M_i})$$

- The quality of the fit is calculated from the merit function

$$F_m = \sum_i (\frac{O_i - M_i}{M_i})$$

k-ω diagram

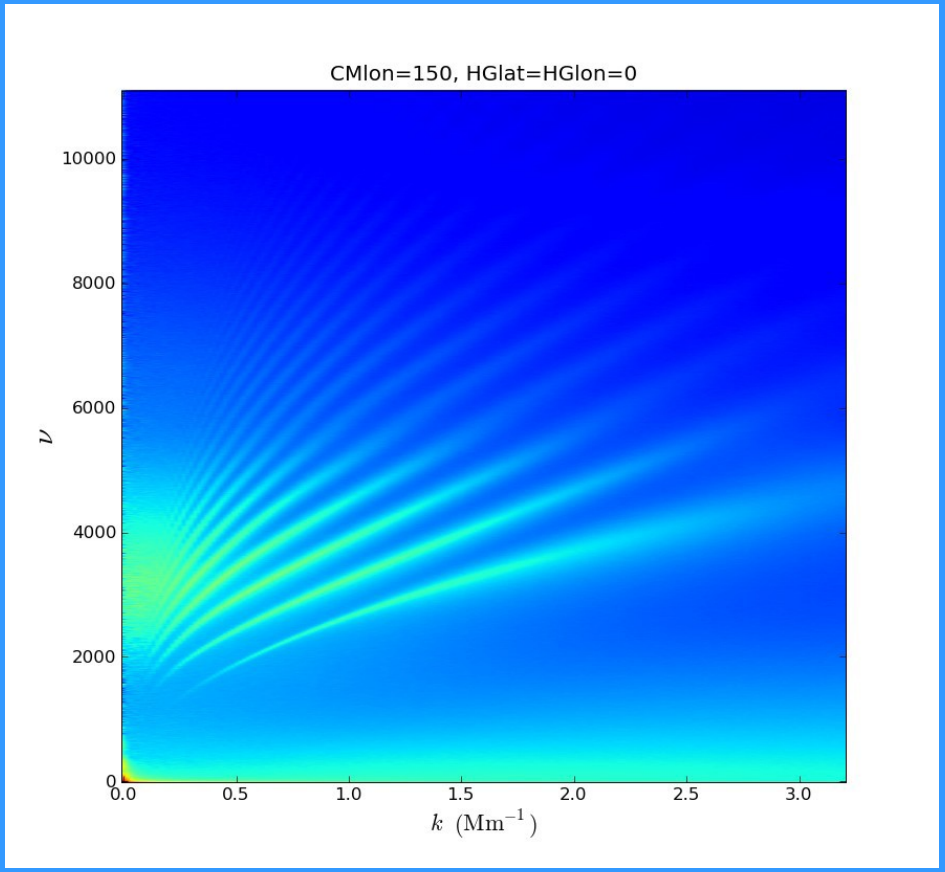
CMlon=150, HGlat=HGlon=0
10000
8000
6000
4000
2000
0
ν
0.0
0.5
1.0
1.5
2.0
2.5
3.0
k (Mm^{-1})

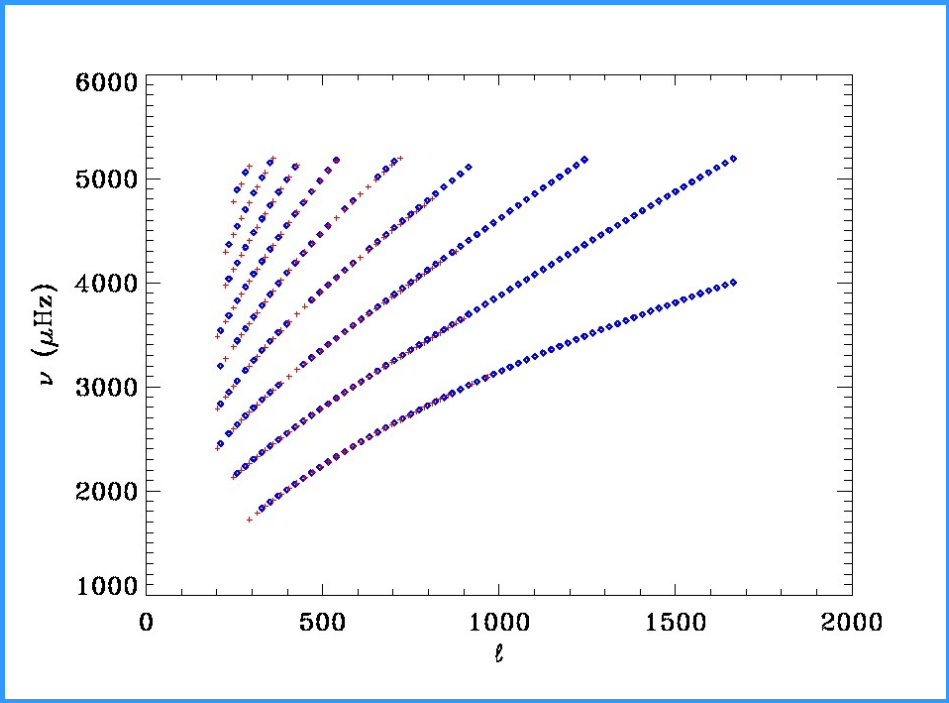
6000
5000
4000
3000
2000
1000
ν (μHz)
0
500
1000
1500
2000
ℓ

HMI Processing

- In the r-d, we normally process a fixed number of regions which are called dense-pack.

- For GONG and MDI, a dense pack consists of 189 regions of 15˚x15˚ patches covering ±60˚ in latitude and longitude, with 50% overlapping

- In HMI, the standard ring products are 5, 15 and 30 degree patches; 282 patches of 15 degrees and covers up to 75˚ in latitude when the observations are favorable

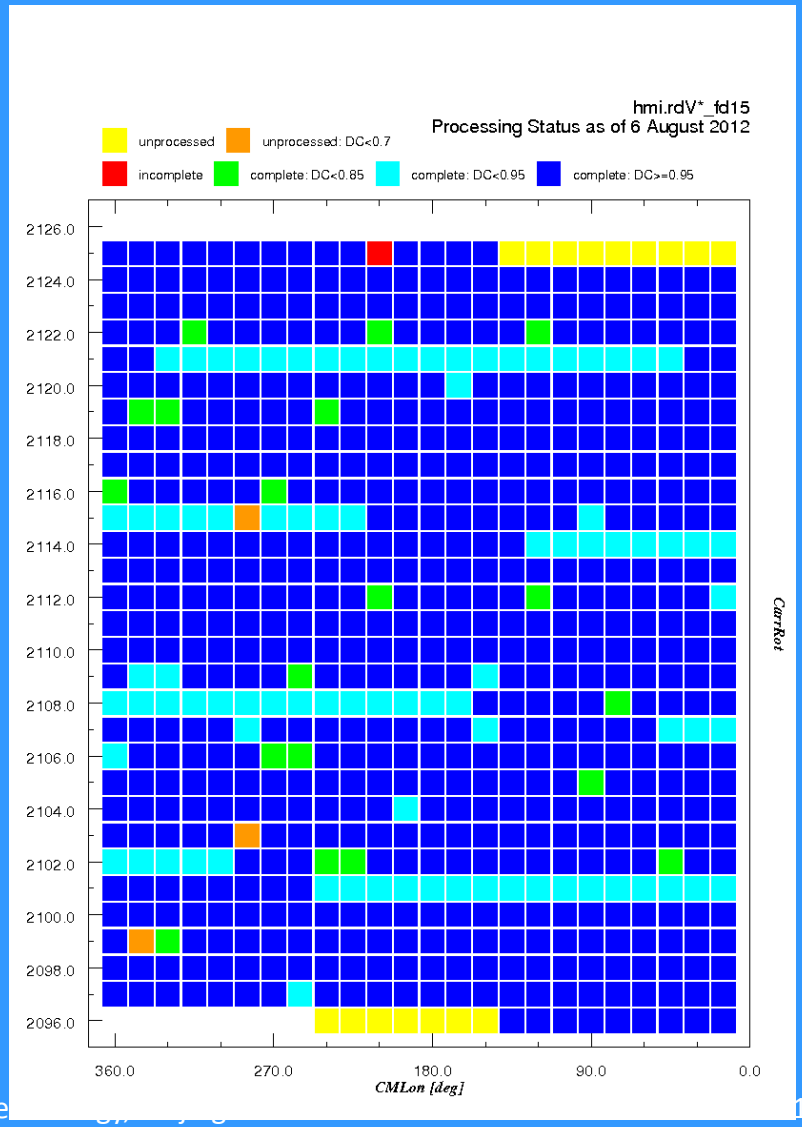

HMI 5 degree Processing

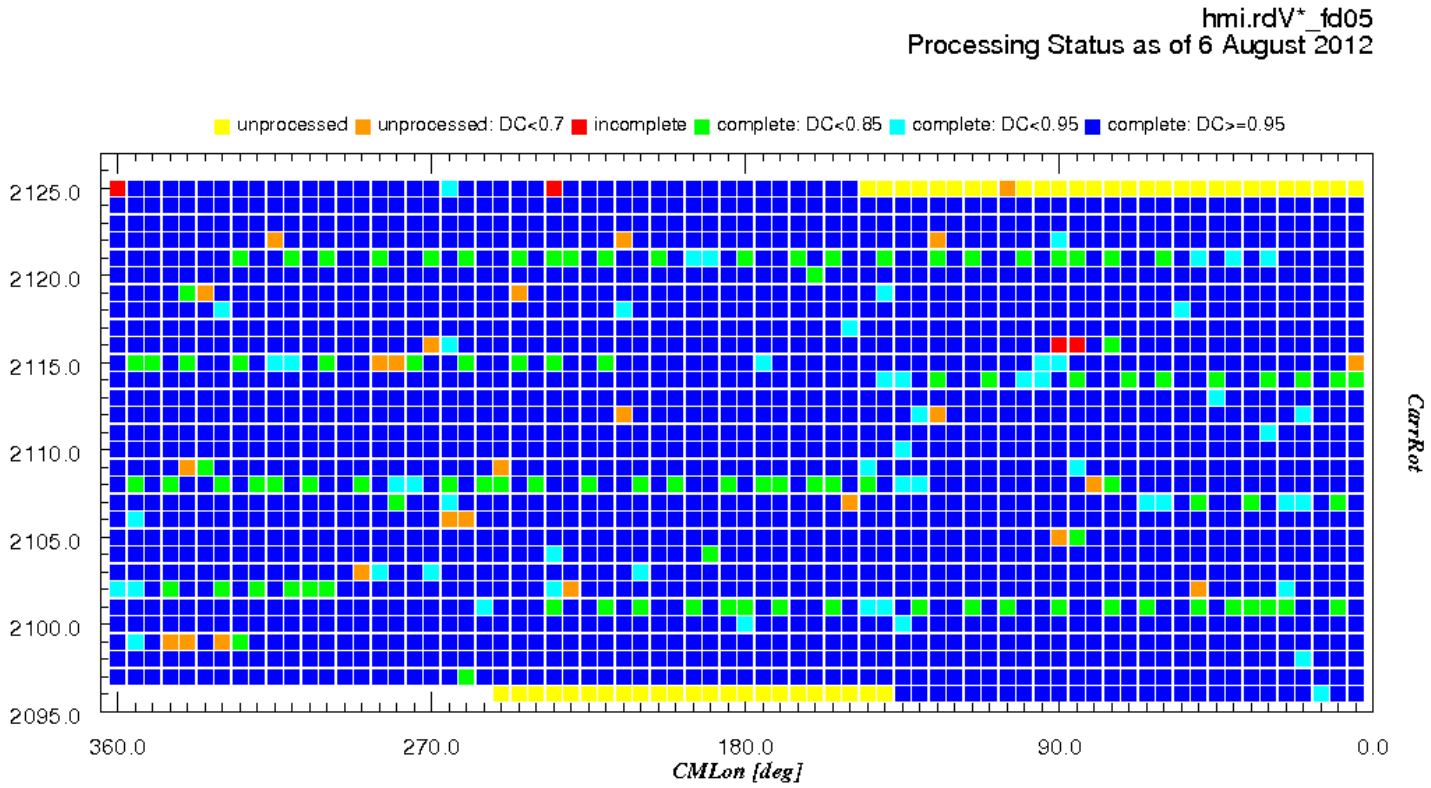

Variation in Mode Parameters

- In the presence of strong surface magnetic fields, such as active regions, the mode parameters (frequencies, amplitudes, line widths) are affected.
- The strength of the magnetic field is measured as Magnetic Activity Index (MAI) . This is calculated by mapping and tracking the magnetograms similar to Dopplergrams for the same duration and averaging the absolute values of the field values ≥ 50 G

Local Frequency shifts during high-activity period

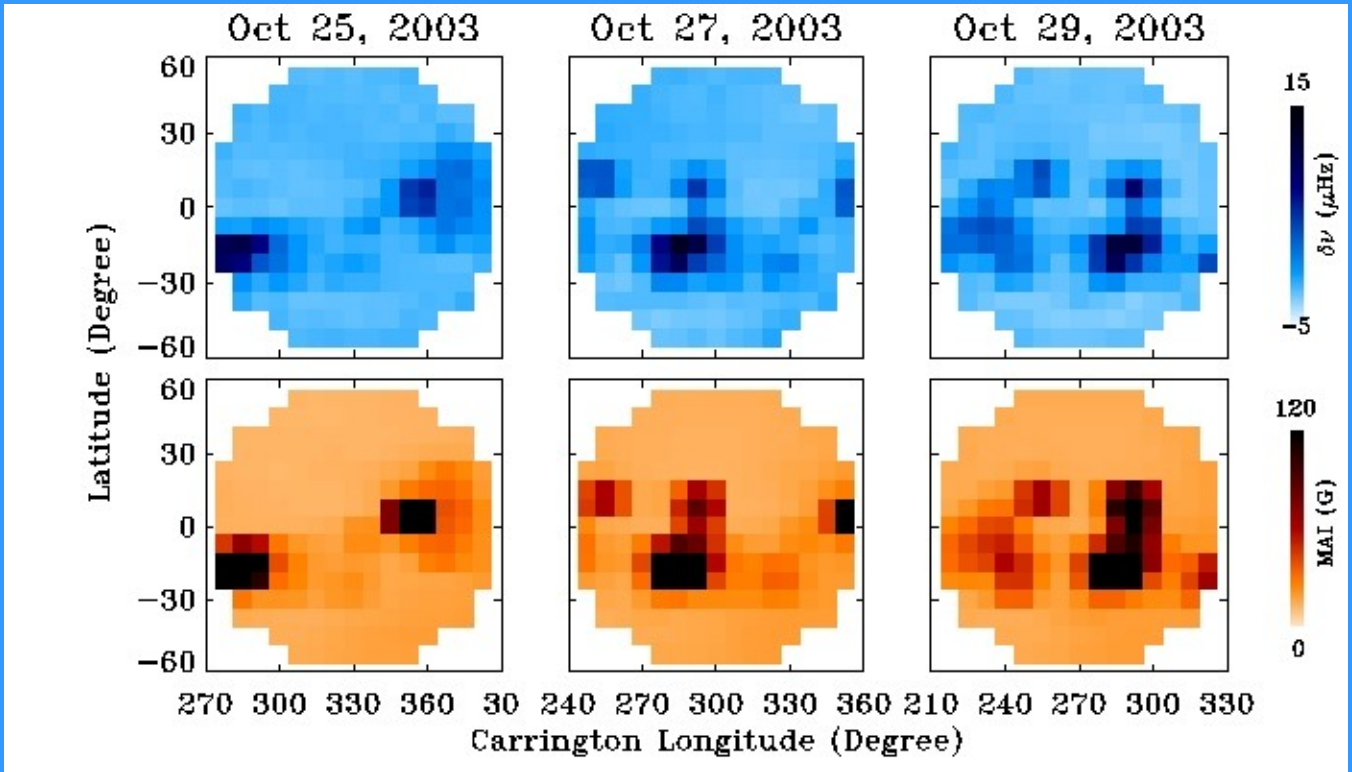

Frequencies act as a tracer of magnetic field

Variation in mode parameters

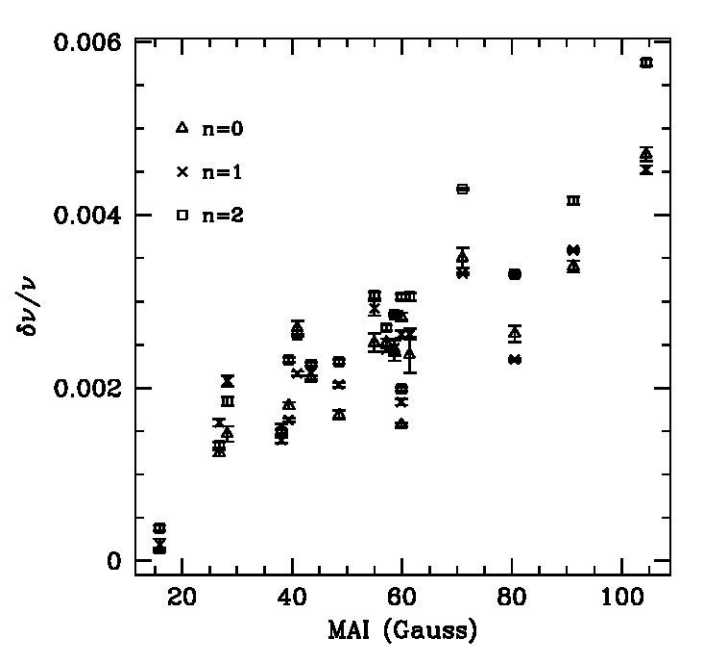

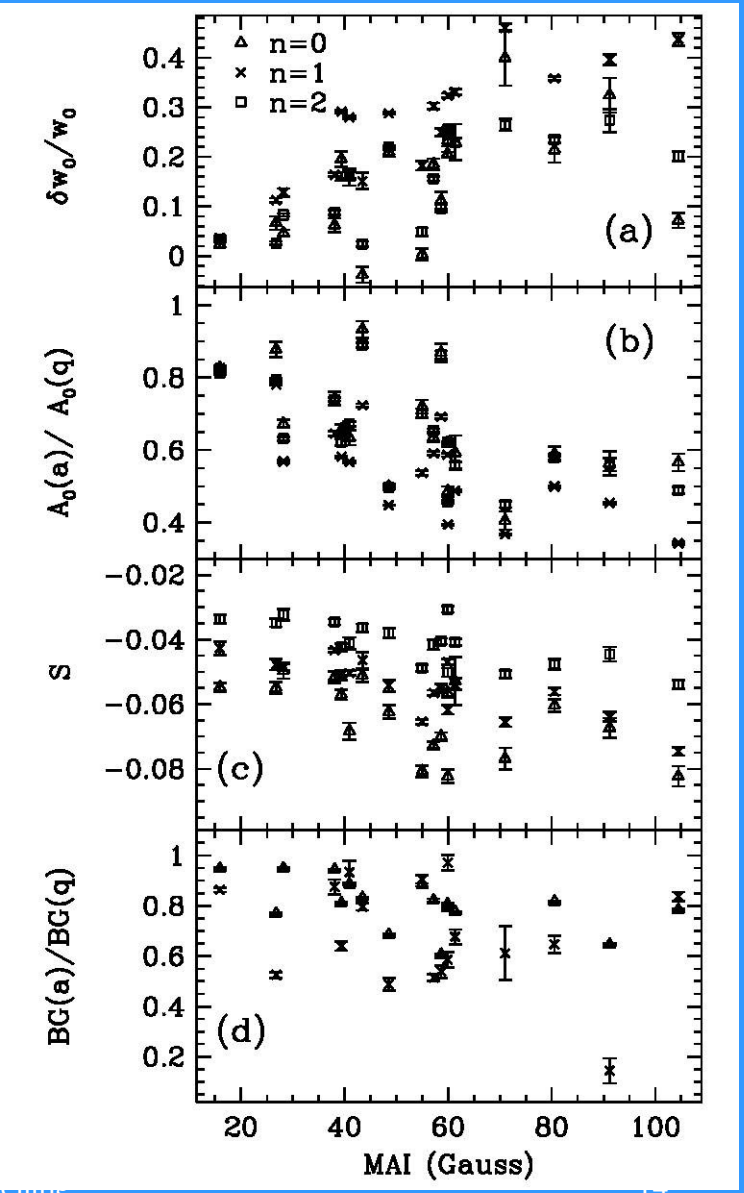

Rajaguru et al. (2003)

Variation in mode parameters

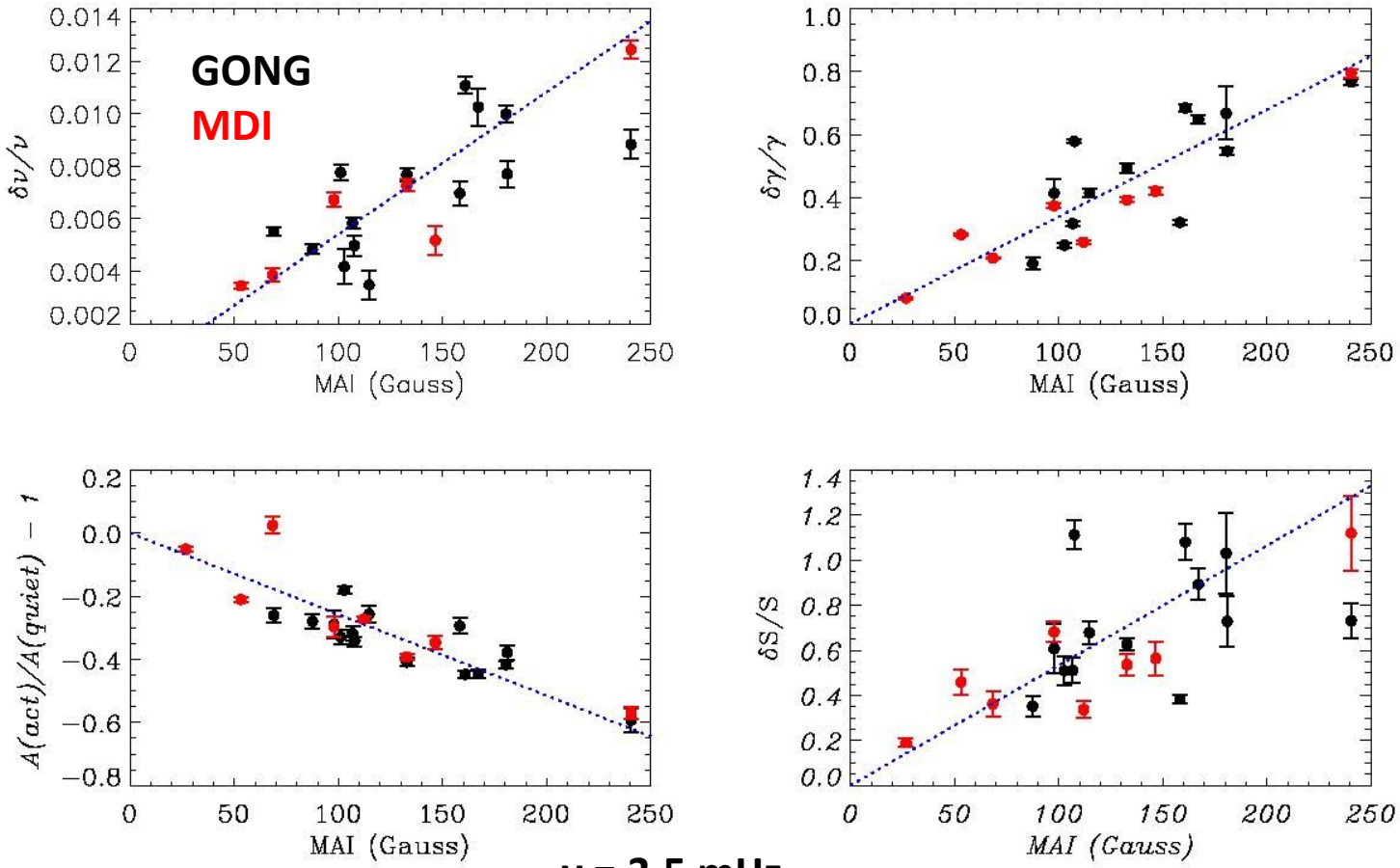

Variation in mode parameters

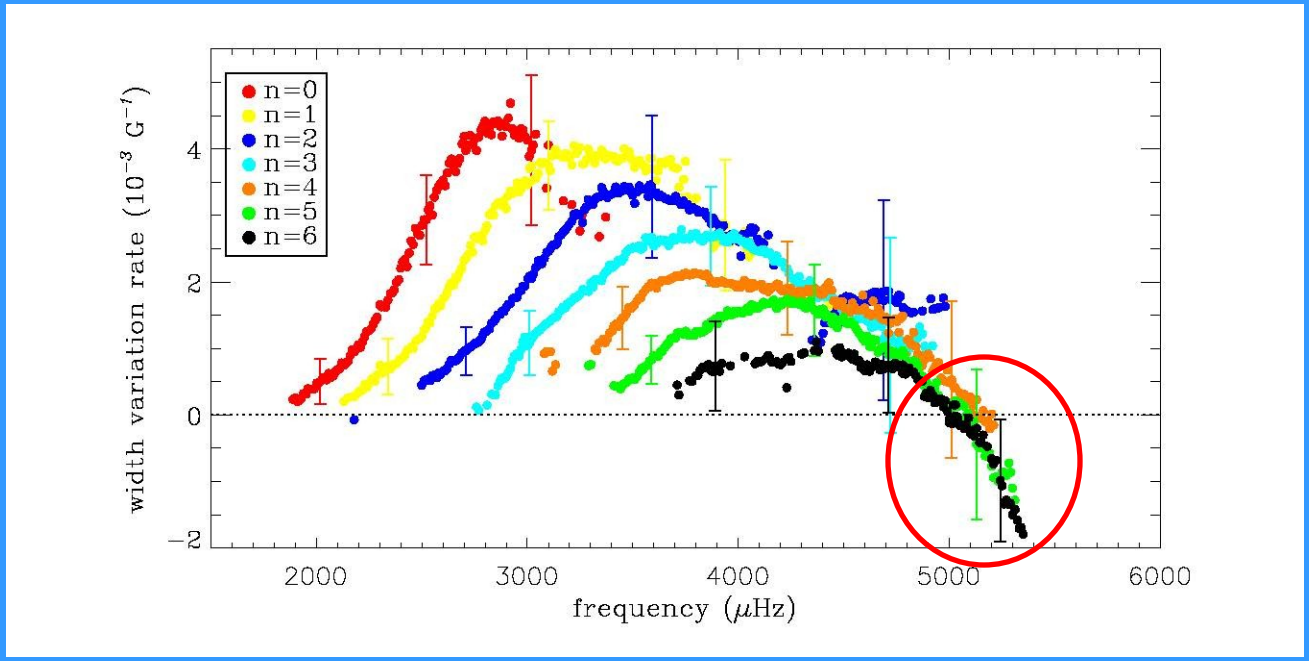

The modes above ν ≥ 5 mHz have a larger lifetime inside the sunspots than outside

Solar cycle variation

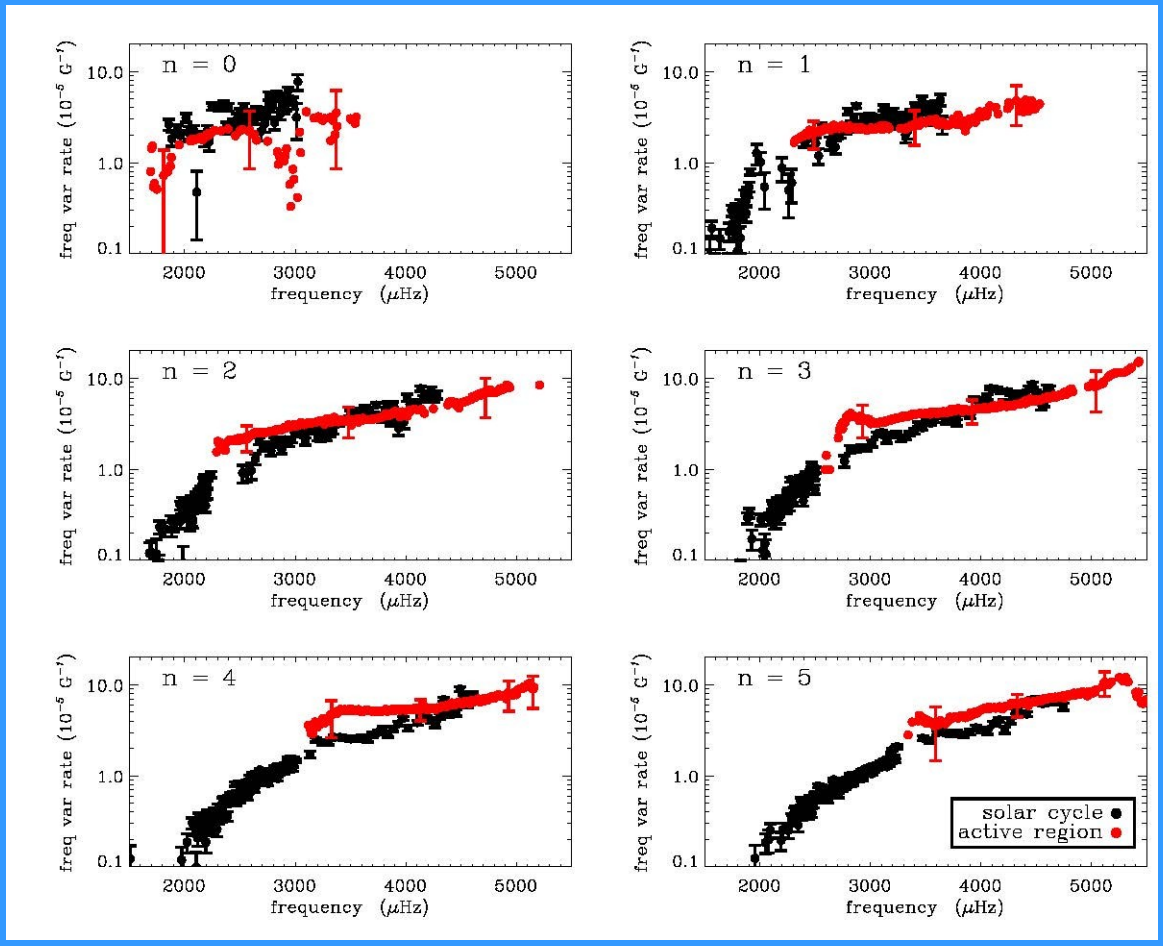

The frequency variation between the active and quite region follows the same power law as the global frequency shifts

Activity Related Variation during solar minimum

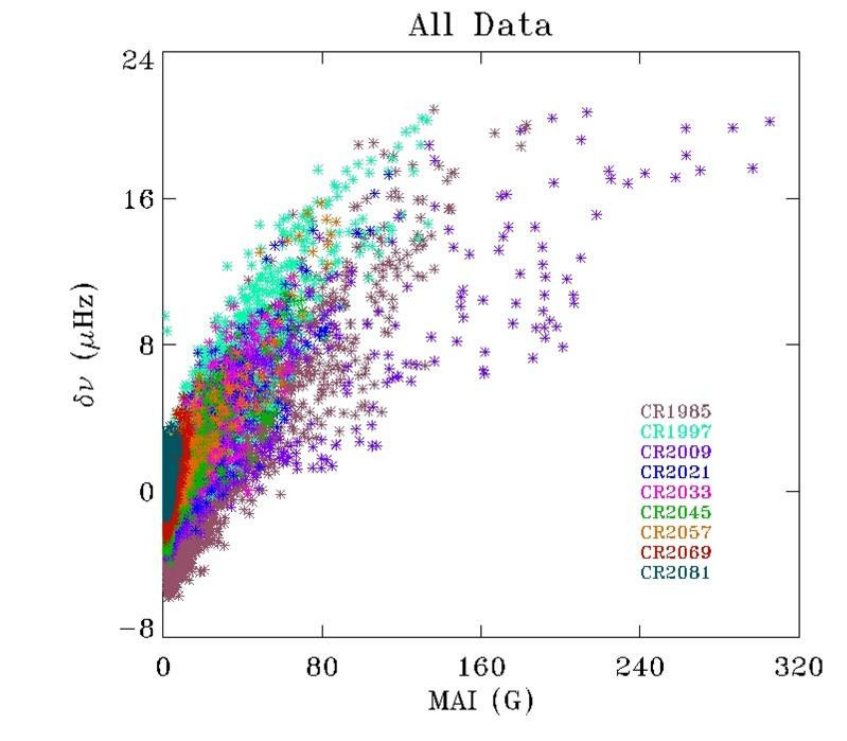

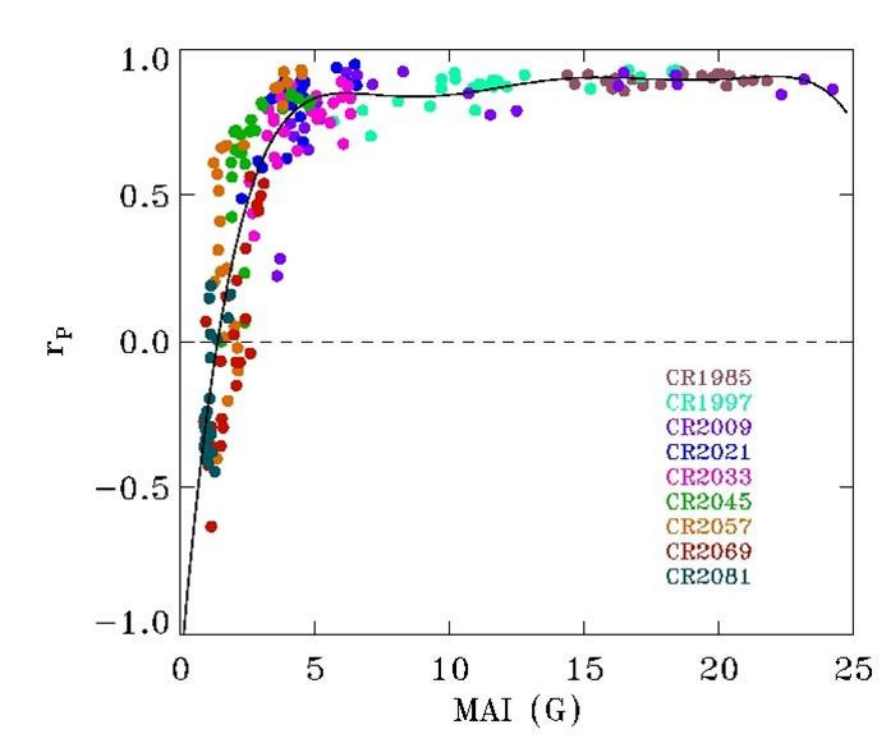

During solar minima, the frequency shifts are weakly correlated with activity

Local Frequency shifts with MAI

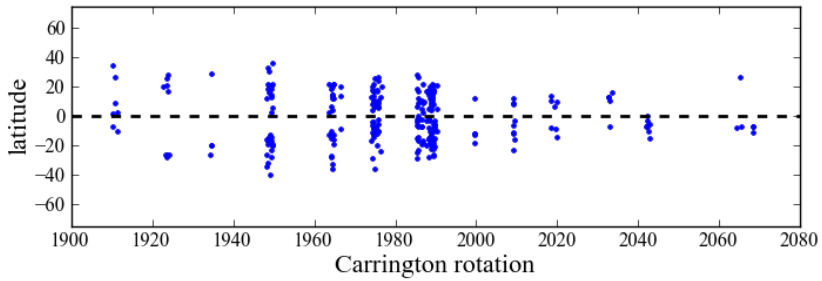

264 Active regions using MDI data

Frequency differences are between a pair of active and two quiet regions at the same latitude and near the time.

Blue and Red symbols indicates unipolar (alpha) and simple bi-polar sunspots (beta).

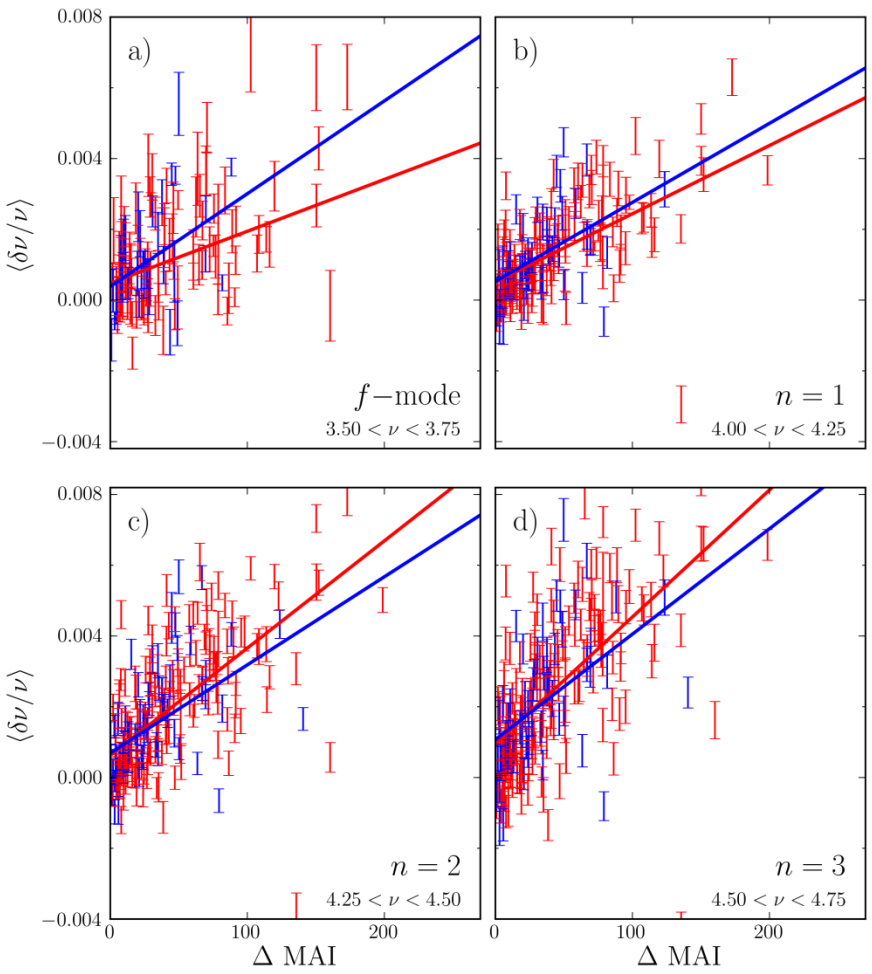

Baldner et al. 2011

Sound Speed Profile

- The frequency differences between a pair of active and quiet region can be inverted to find the thermal structure of the near surface layers

$$\frac{\partial \varpi_i}{\varpi_i} \approx \int_0^R K^i_{c^2,\rho}(r) \frac{\partial c^2}{c}(r) dr$$

Example of sound speed

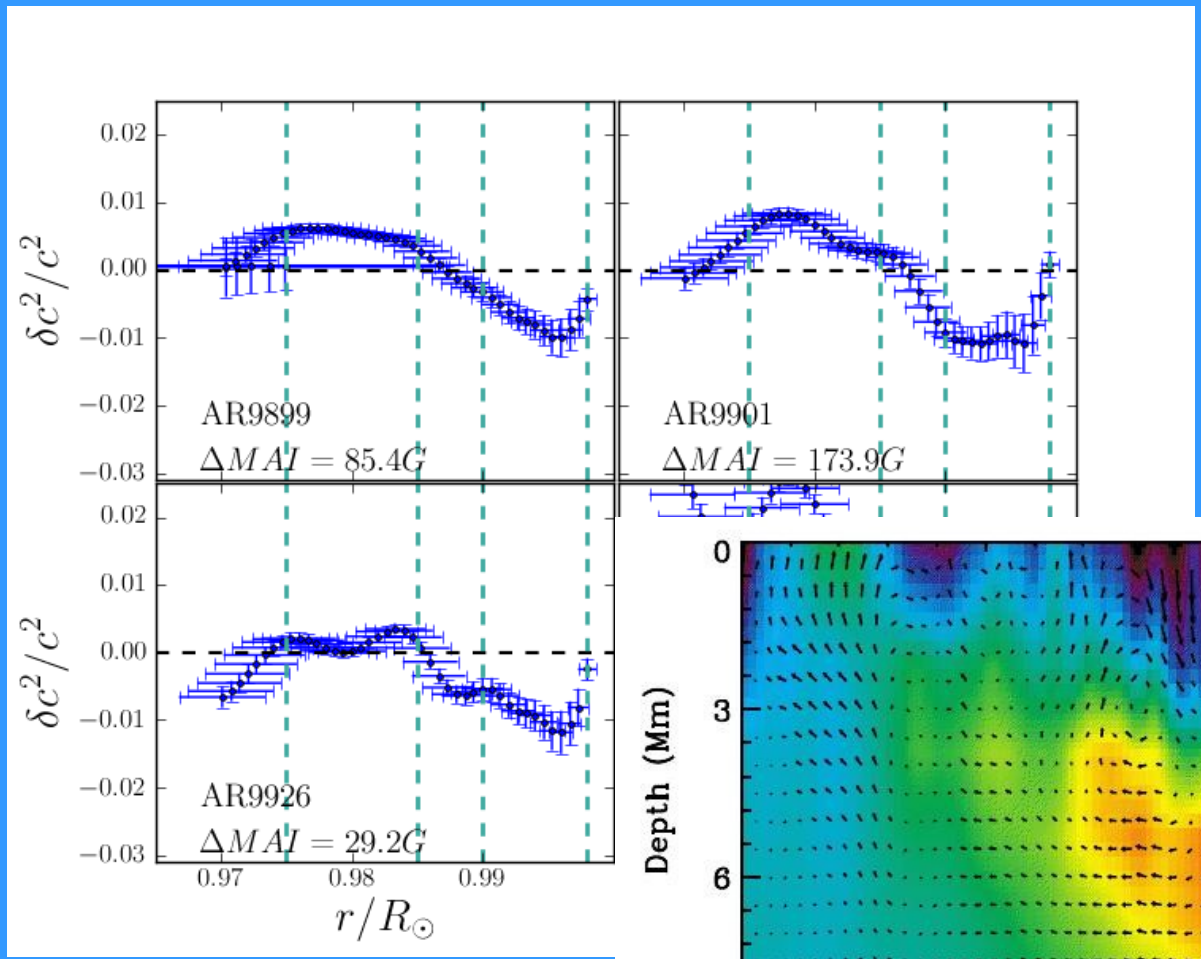

A two-layer structure is visible:
Negative perturbation in the outer layer and a Positive perturbation in the deeper layer

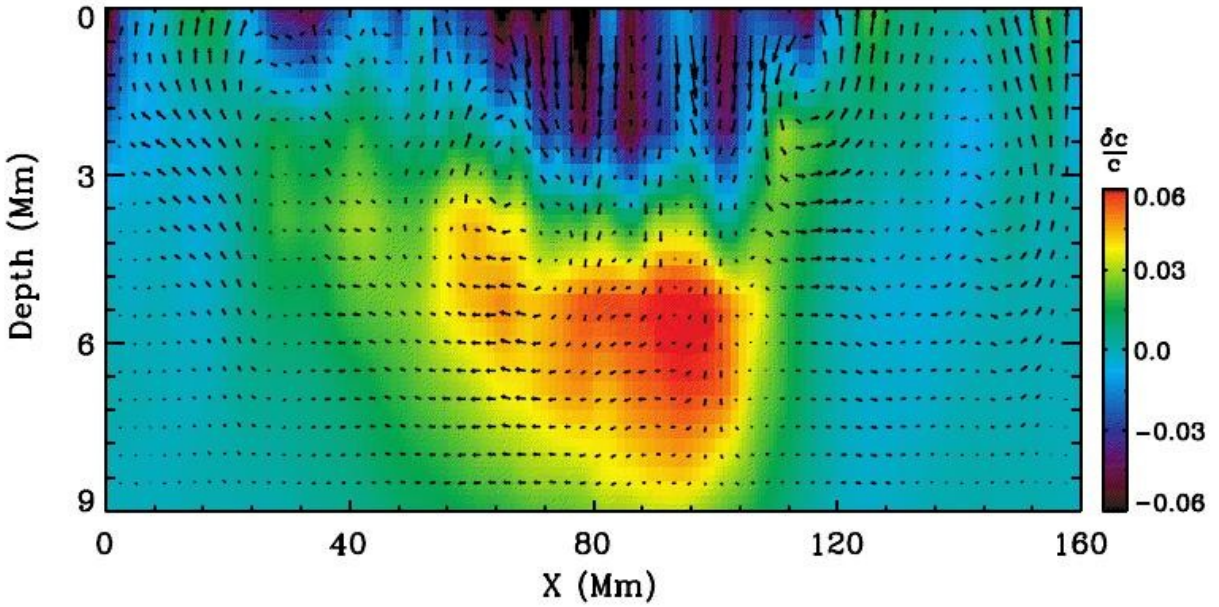

Baldner et al.

Examples from HMI

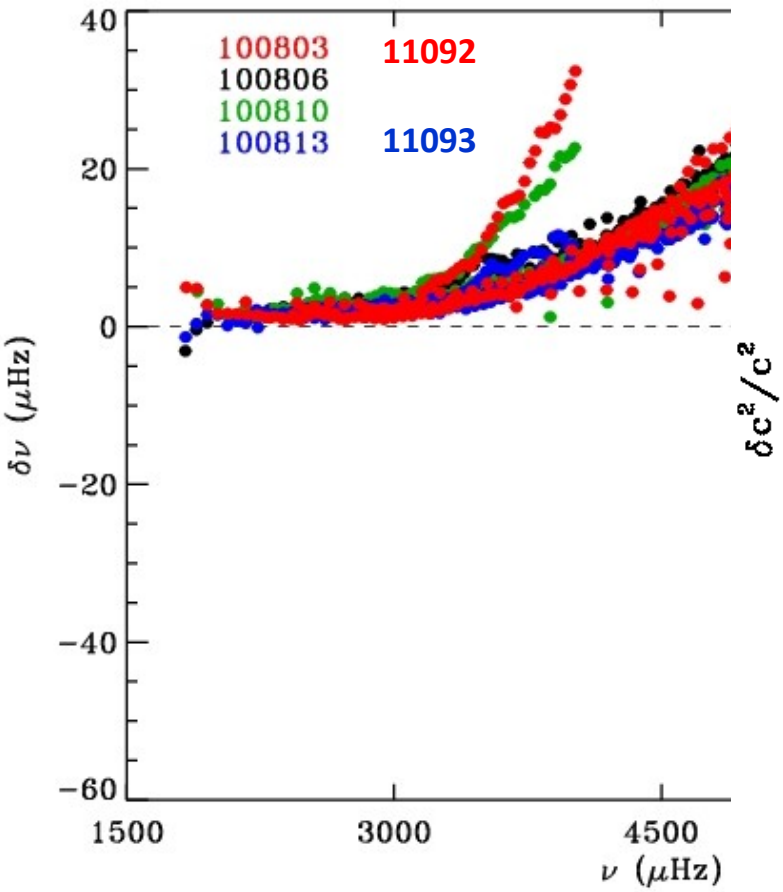

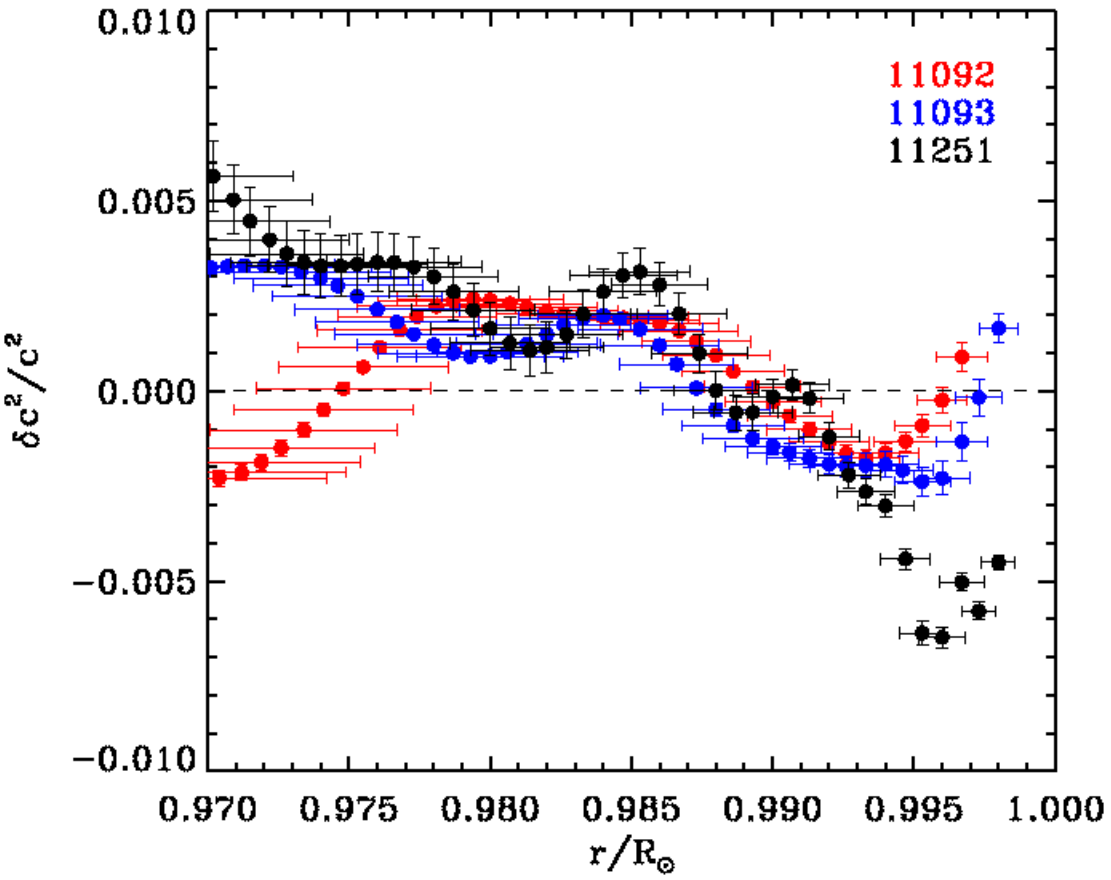

Sound speed

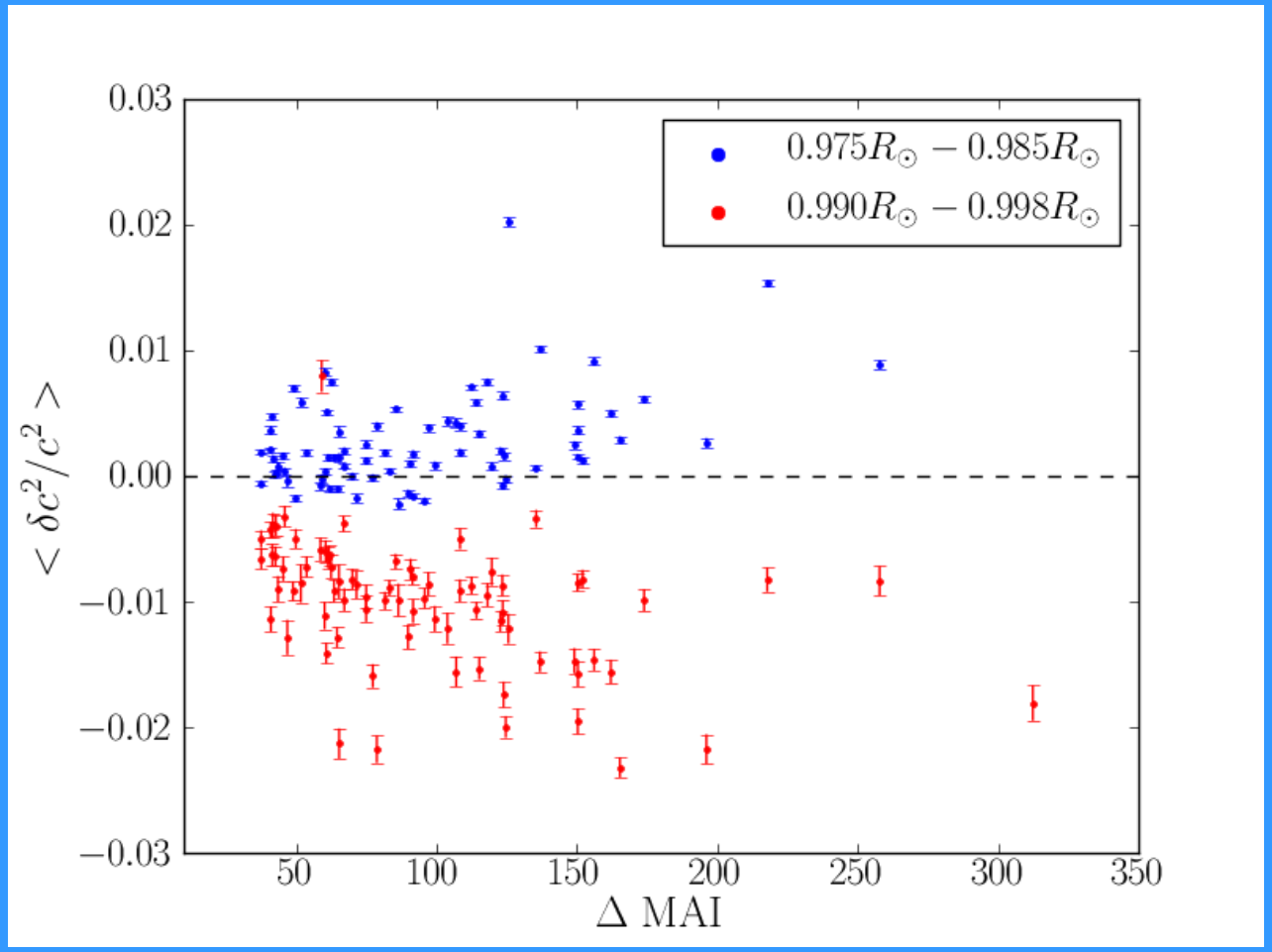

Baldner et al. (2011)

The magnitude of the perturbations, both negative and positive increase with increasing MAI

Example of sound speed kernel

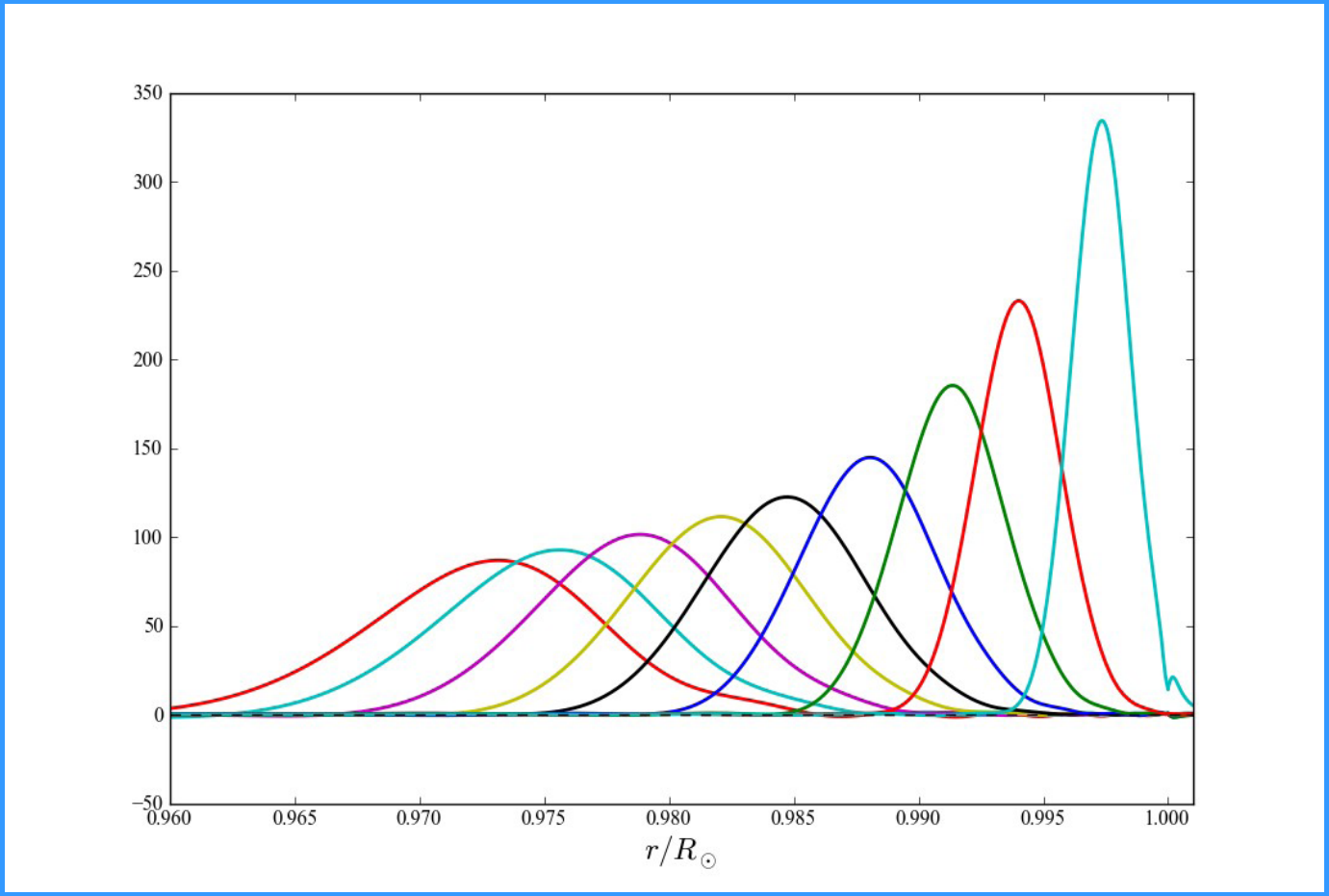

Boundaries between perturbations

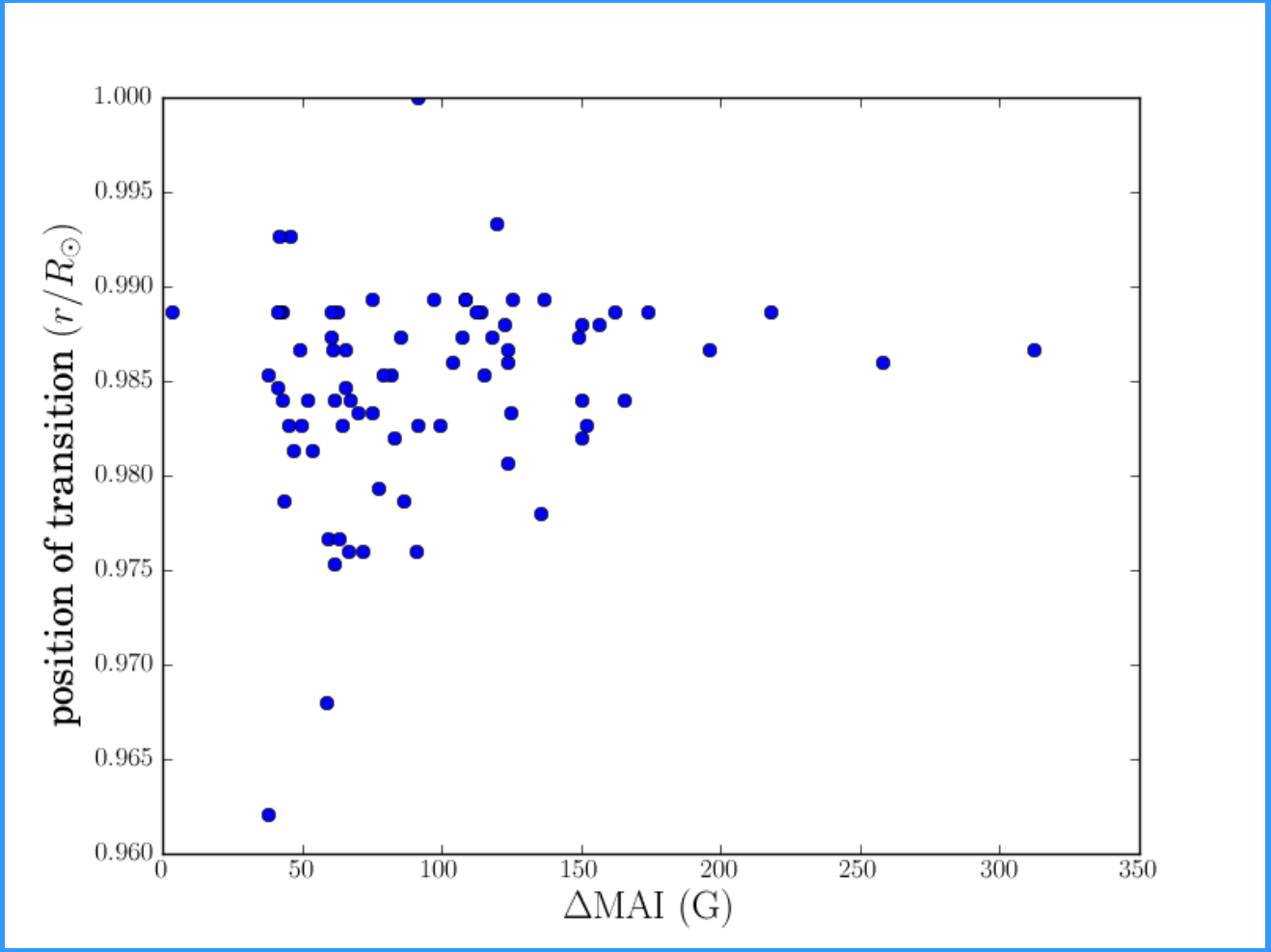

Sound Speed Profile

- The frequency differences between a pair of active and quiet region can be used to find the thermal structure of the near surface layers
- The general consensus from r-d is that the sound speed has a two layer profile: depressed between 3Mm (0.995R) and 7 Mm (0.99) and enhanced in the deeper layer (11-21 Mm)
- The magnitude of the perturbations, both negative and positive increase with increasing MAI

Discrepancy between ring and time-distance result (AR 9787)

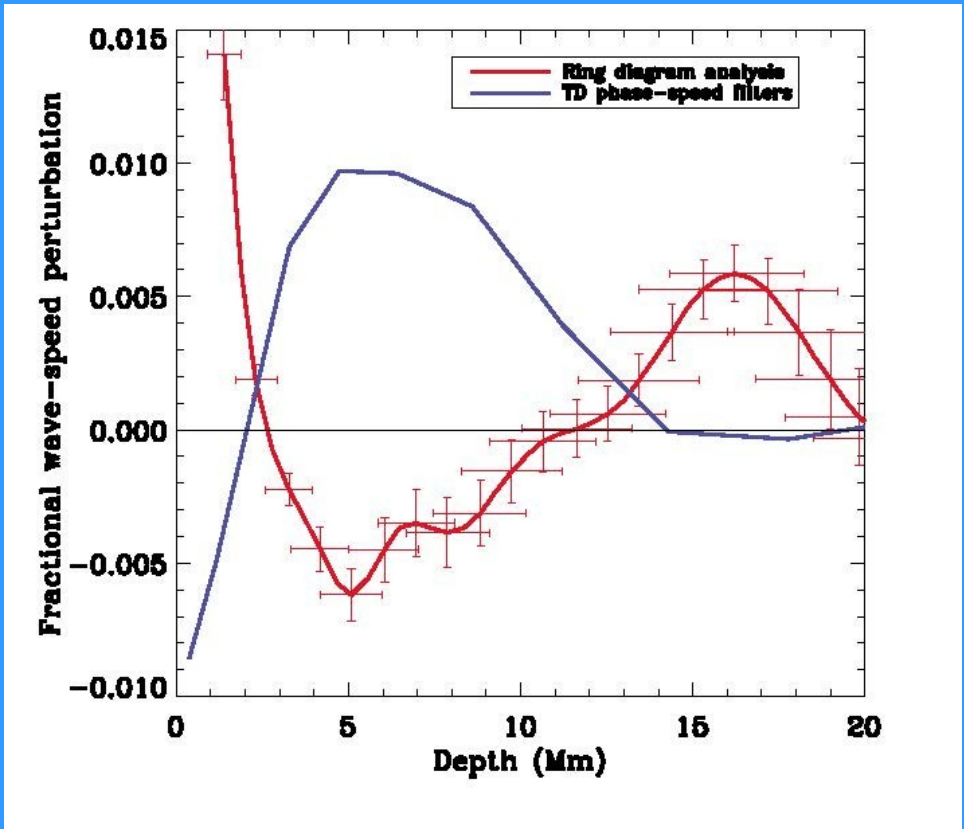

Wave/sound speed deduced under the active region NOAA 9787 using the local helioseismic techniques of time–distance helioseismology (blue) and ring analysis (red). The two techniques produce opposite inferences. The reason is probably the incomplete understanding of the physical modeling of the wave field (Gizon et al., 2009)

SUB-SURFACE FLOWS

Fitting Technique

- Quantitative analysis of ring-diagrams are undertaken by fitting model spectra profiles to the data.
- Two types of models are normally used: a symmetric Lorentzian and an asymmetric profile:

$$P = \frac{A\Gamma}{(\omega - \omega_0 + k_x U_x + k_y U_y)^2 + \Gamma^2} + \frac{b_0}{k^3}$$

$$P(k_x, k_y, \nu) = \frac{e^{B_1}}{k^3} + \frac{e^{B_2}}{k^4} + \frac{exp(A_0 + (k - k_0)A_1 + A_2(k_x/k)^2 + A_3\frac{k_x k_y}{k^2})S_x}{x^2 + 1}$$

where

$$x = \frac{\nu - ck^p - U_x k_x - U_y k_y}{w_o + w_1(k - k_0)}$$

$$S_x = S^2 + (1 + Sx)^2$$

Zonal and Meridional Flows

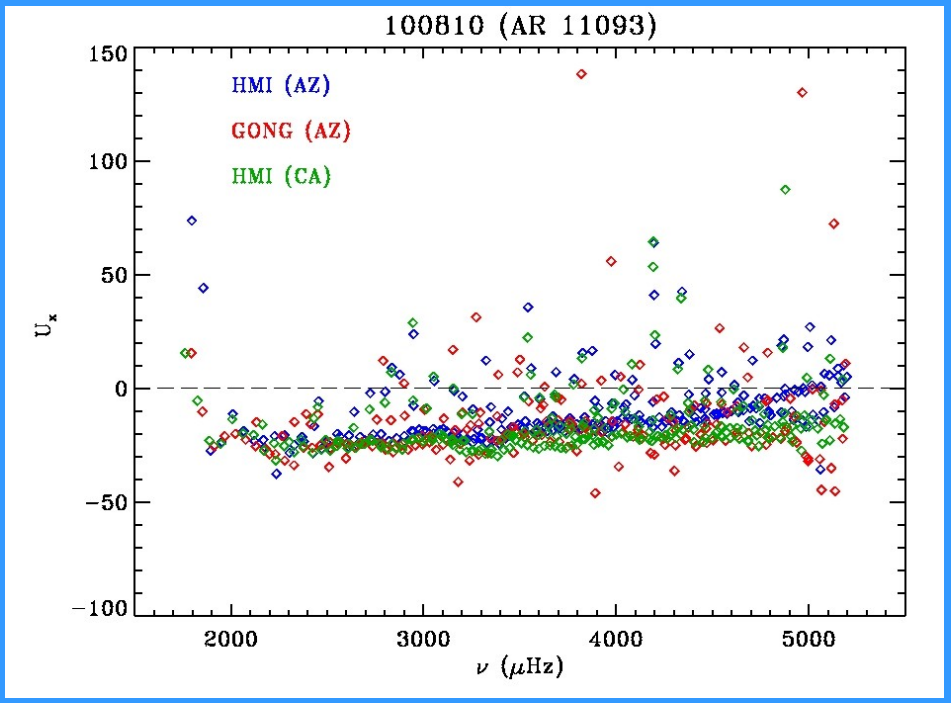

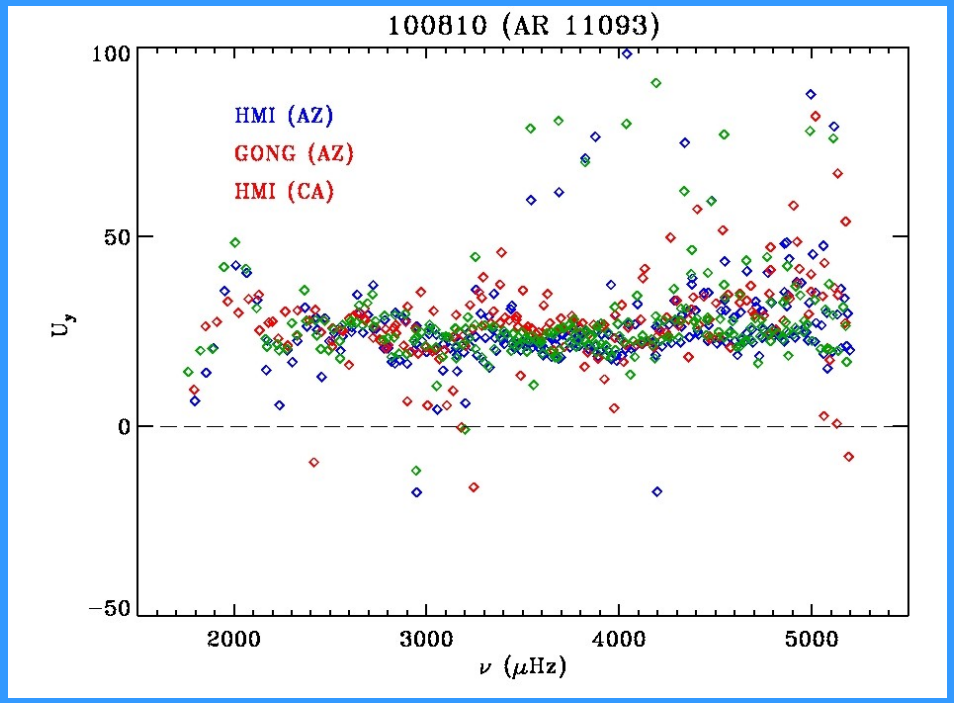

These are inverted to obtain the sub-surface flows

Flow inversions for a single tile

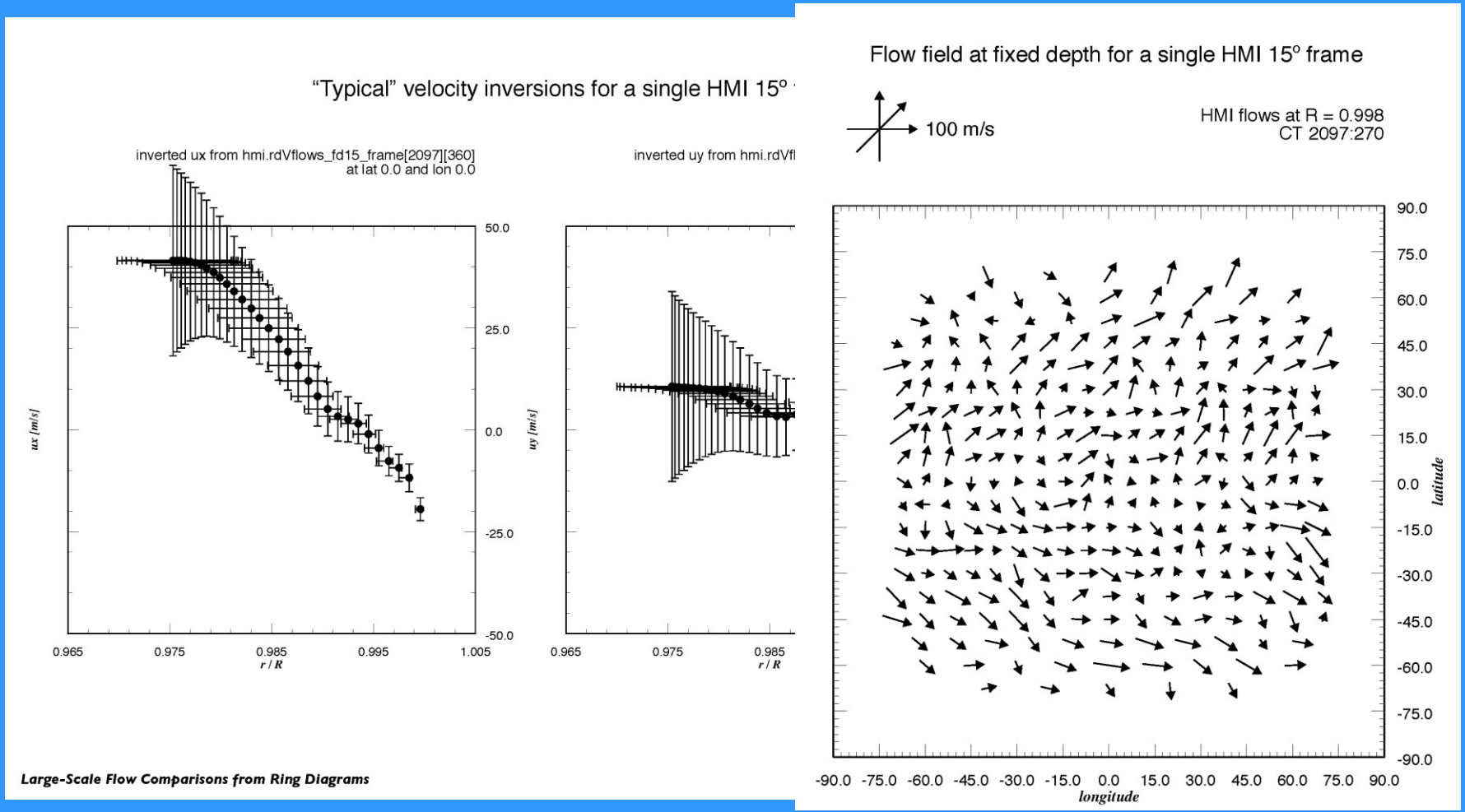

Average zonal and meridional flows at surface

Zonal

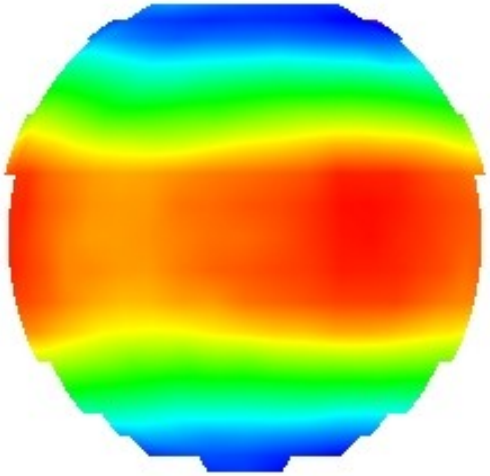

CR 2102

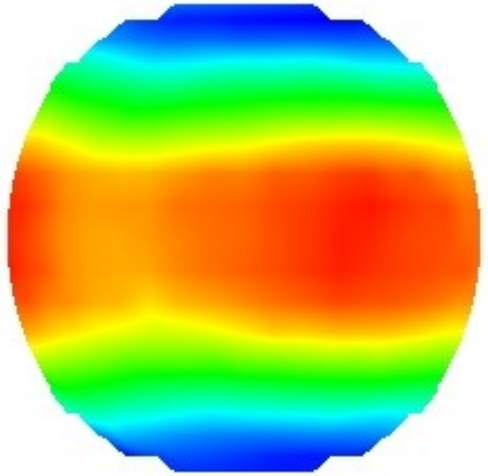

CR 2103

Meridional

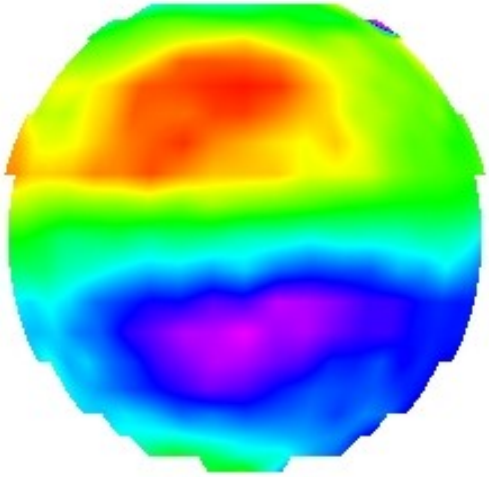

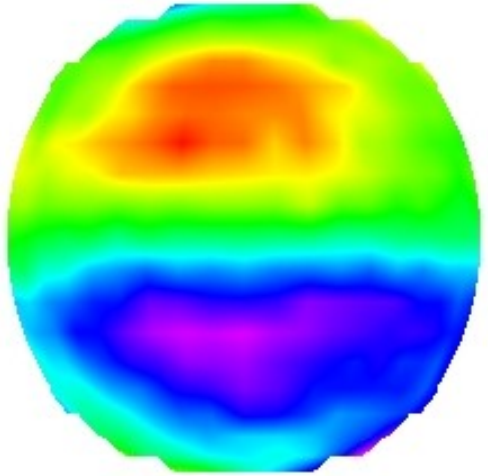

Evolution of Flow in AR 11093

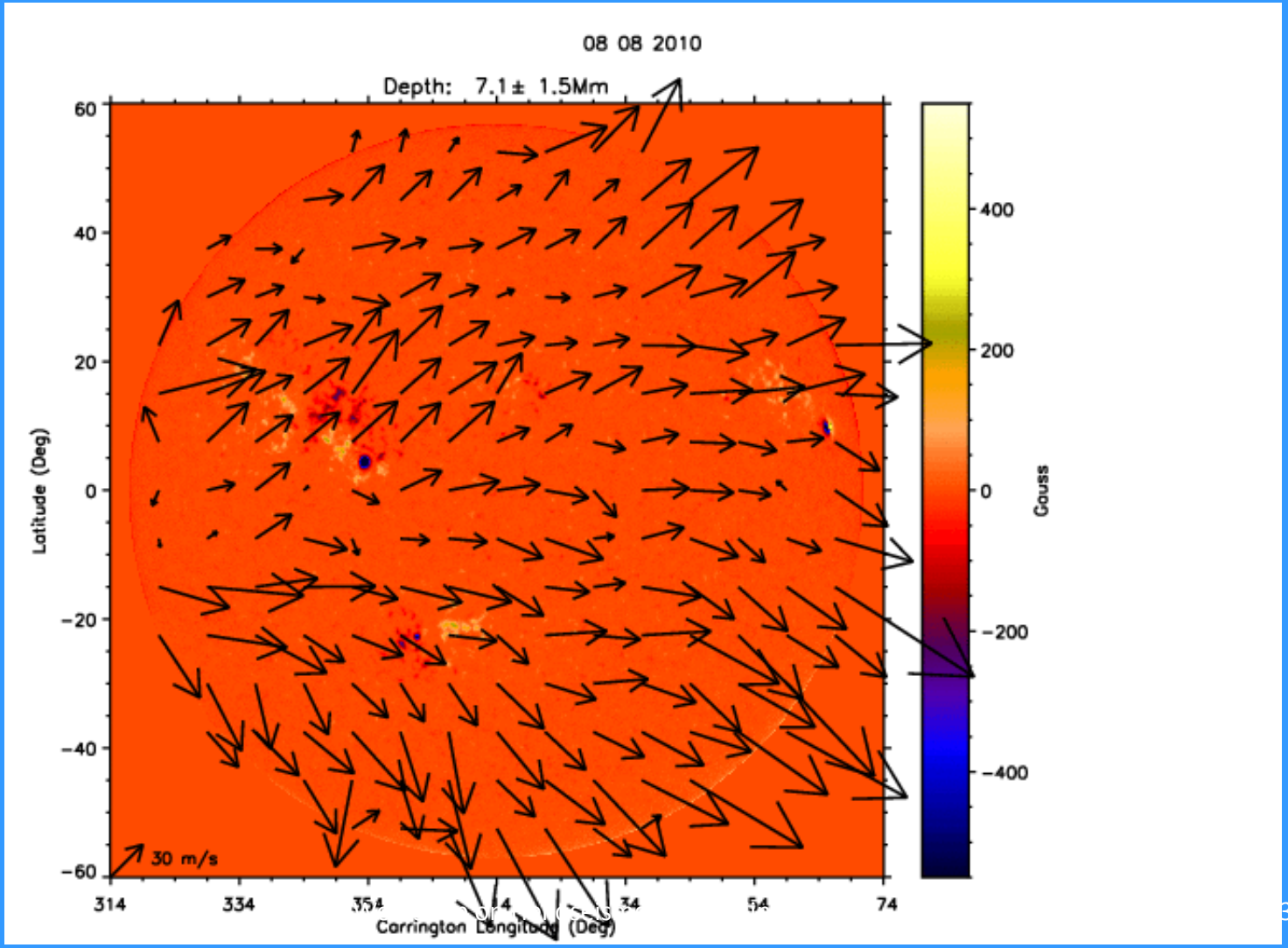

Variation of flow with depth

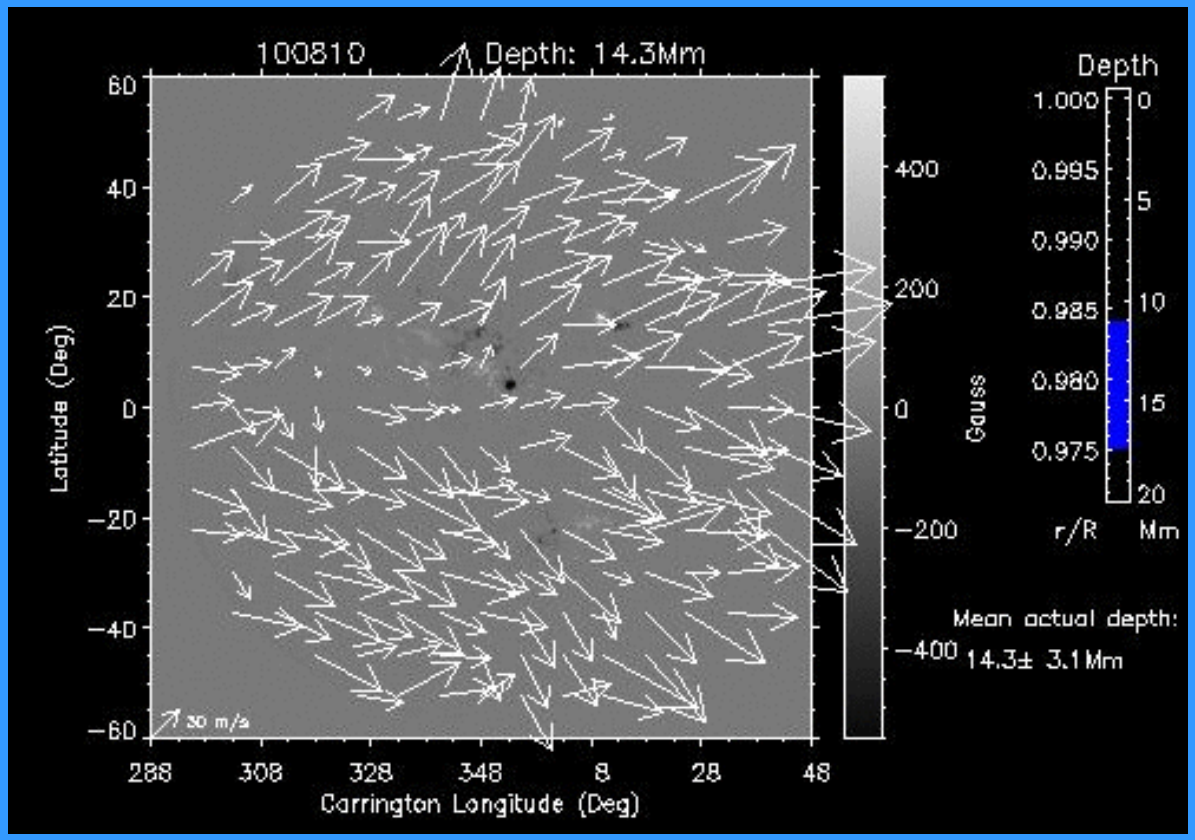

High-resolution Flow Maps

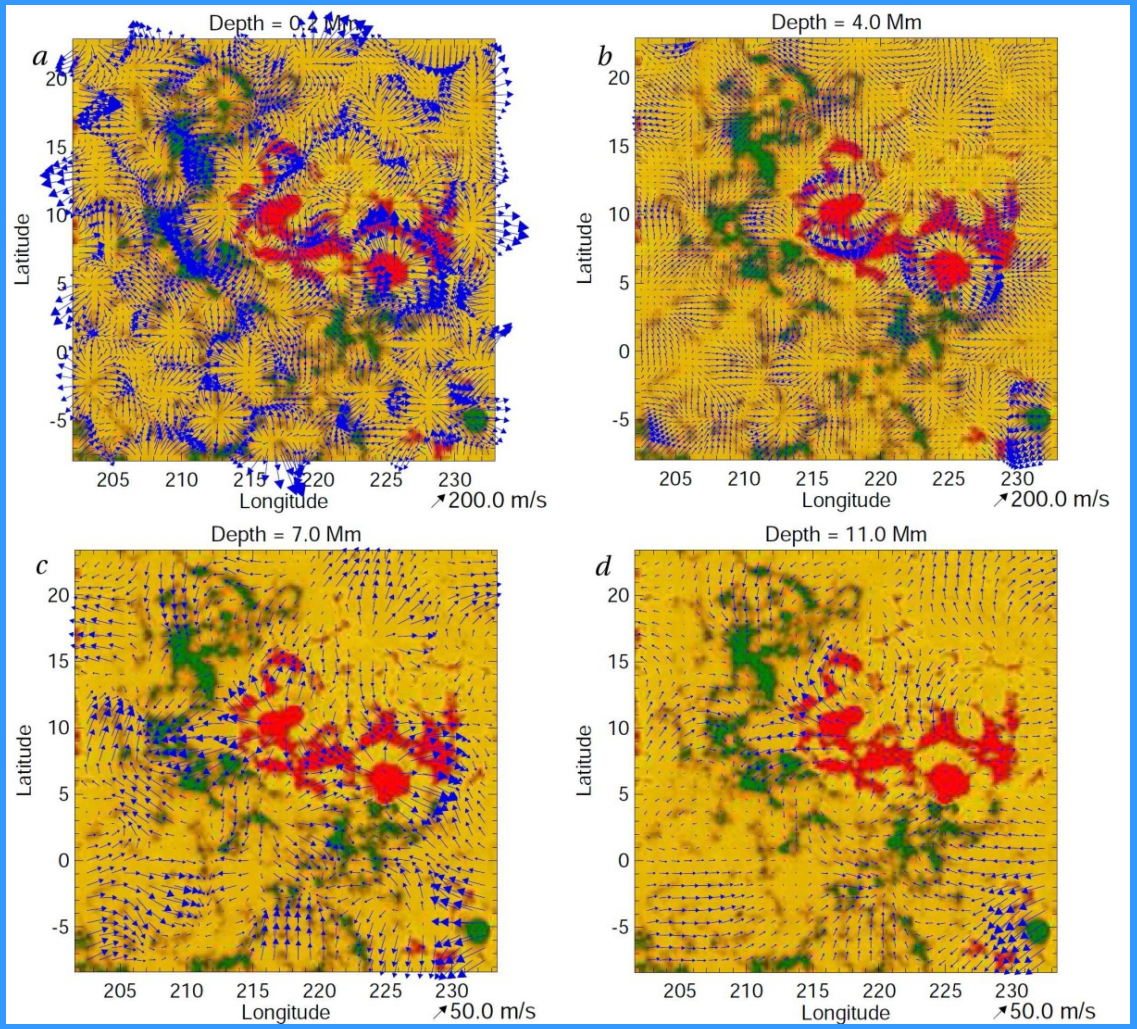

Flow field realized through high-resolution inversion of ring-analysis measurements of MDI obtained in January 2002. Horizontal velocity vectors (**blue**) overlay the magnetogram for that day (positive field in **red**, negative in green). At a depth of 0.2 Mm (a), the cellular structure of supergranulation is apparent. Strong outflows are visible around the two sunspots at longitude 215◦ and 225◦ down to a depth of 7 Mm (b, c). Below 7 Mm (d), flows are decidedly larger scale and exhibit no outflows from the sunspots.

Featherstone et al. (2011)

Flows around active regions

- It is generally found that the strong active regions show convergent horizontal flows close to the surface and divergent flows at greater depth.

Large Scale Meridional Flows
(Averaged over 18 CR from HMI;)

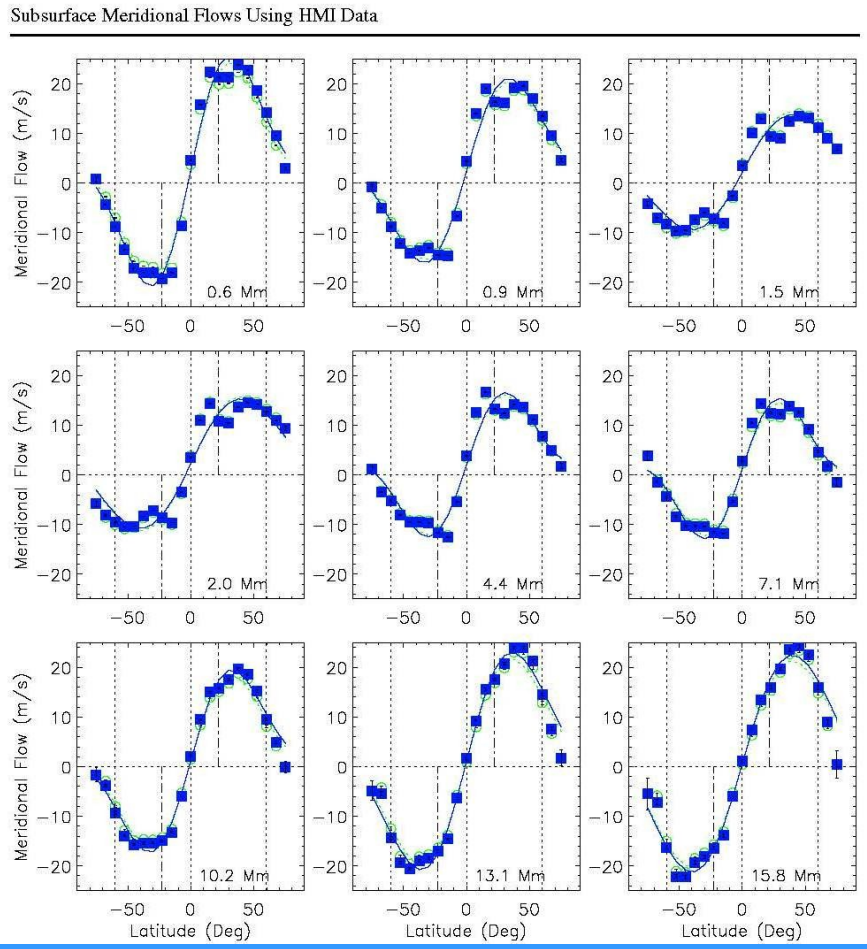

Positive values are flows towards North; negative towards South Pole

Blue line is a fit from first-two even-order Legendre Polynomial

Vertical lines are mean latitude of activity

Counter cells are visible at high latitude and some depths

Komm et al. (2012)

Temporal variation of residual meridional flow (averaged below 5Mm)

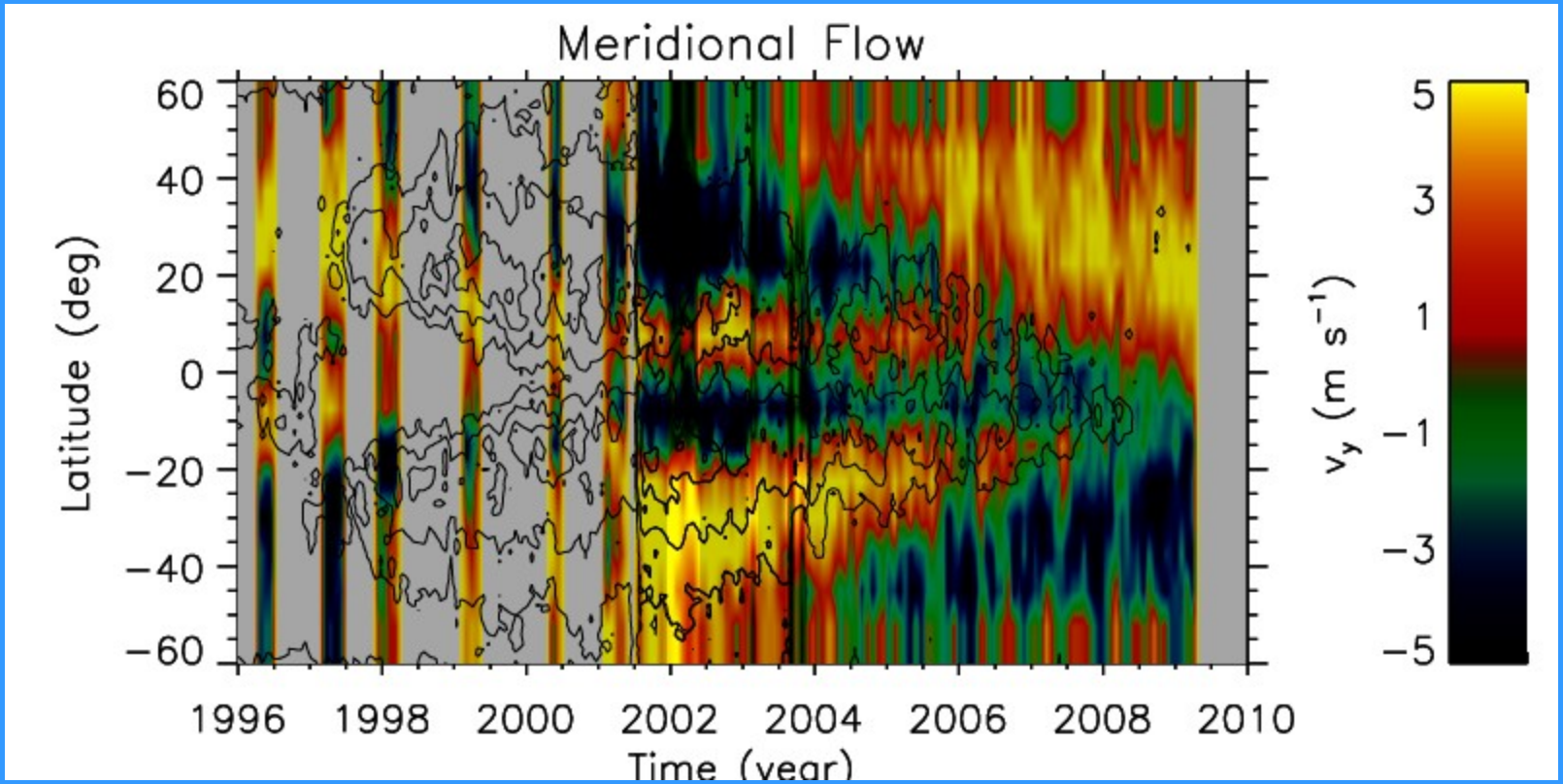

Mean latitudes of magnetic activity are locations of converging flows
The flow pattern appears before magnetic activity (similar to zonal flows)

Solar Cycle variation of Zonal and Meridional Flows

0.9-2 Mm

2 - 10.2 Mm

10.2 - 15.8Mm

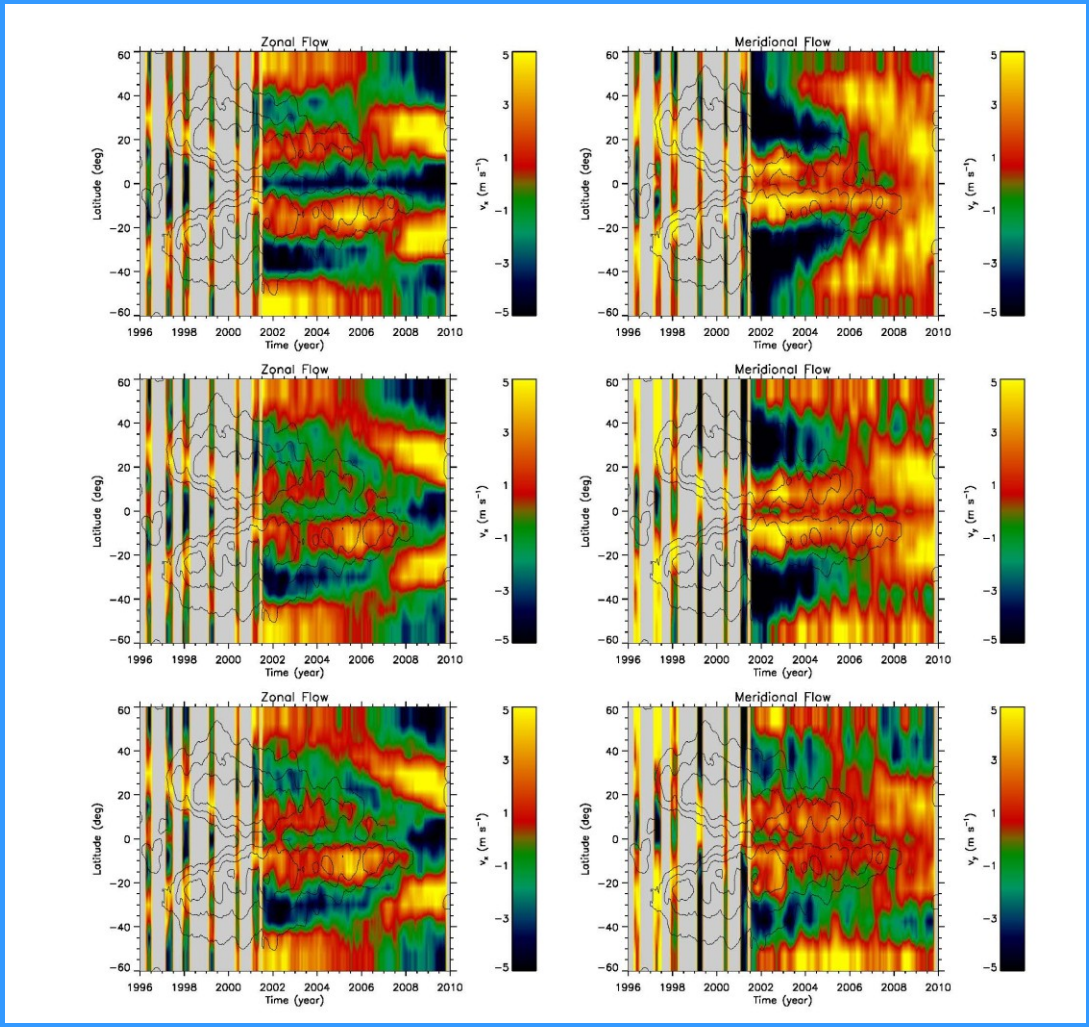

Connection to Space Weather

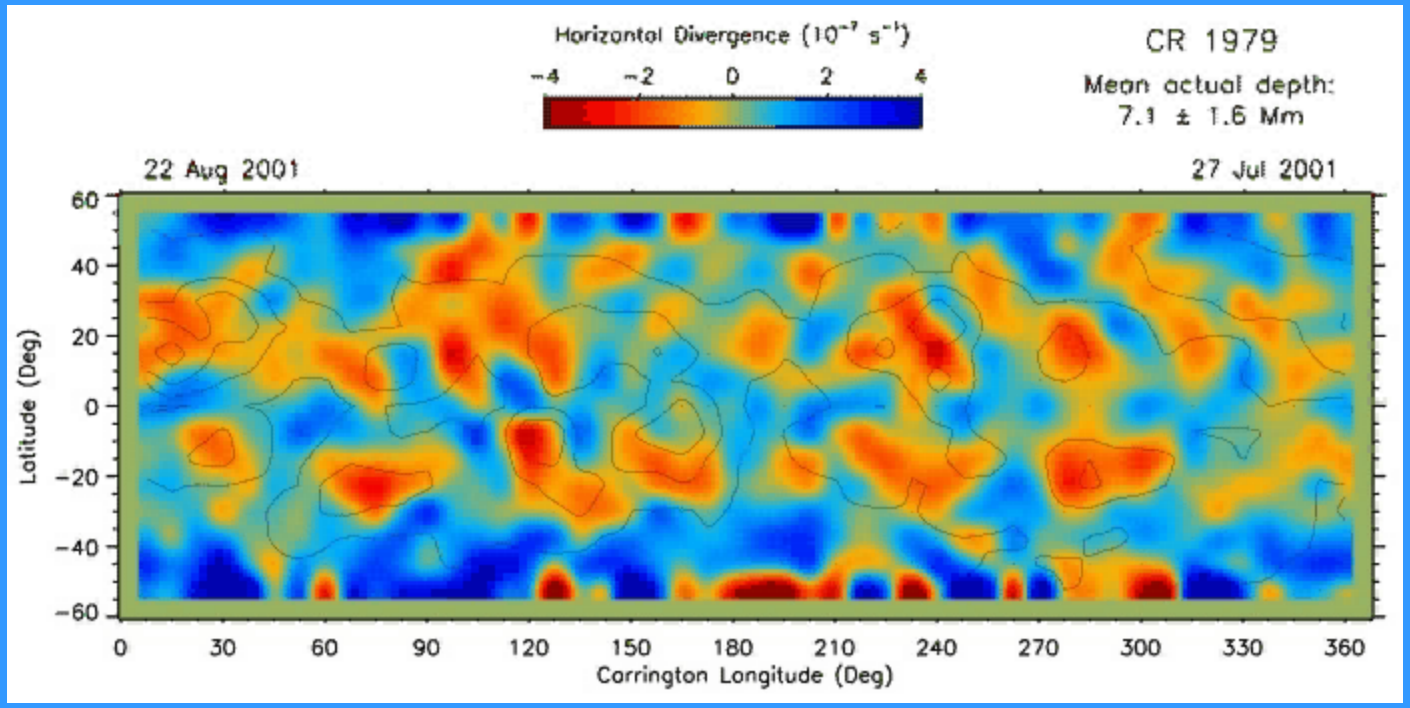

- Sub-surface flow parameters, such as vorticity (curl v) and kinetic helicity density ((curl v).v) have been found to improve the ability to distinguish the flaring and non-flaring activity.

(For details see Komm et al., 2011, Solar Phys., 268)

Multi-height and multi-wavelength ring-diagram

Simultaneous observations at different heights in solar atmosphere allow us to investigate

how the results from helioseismology are affected by the choice of observable and the height of formation of the spectral line in solar atmosphere.

Ring Diagrams

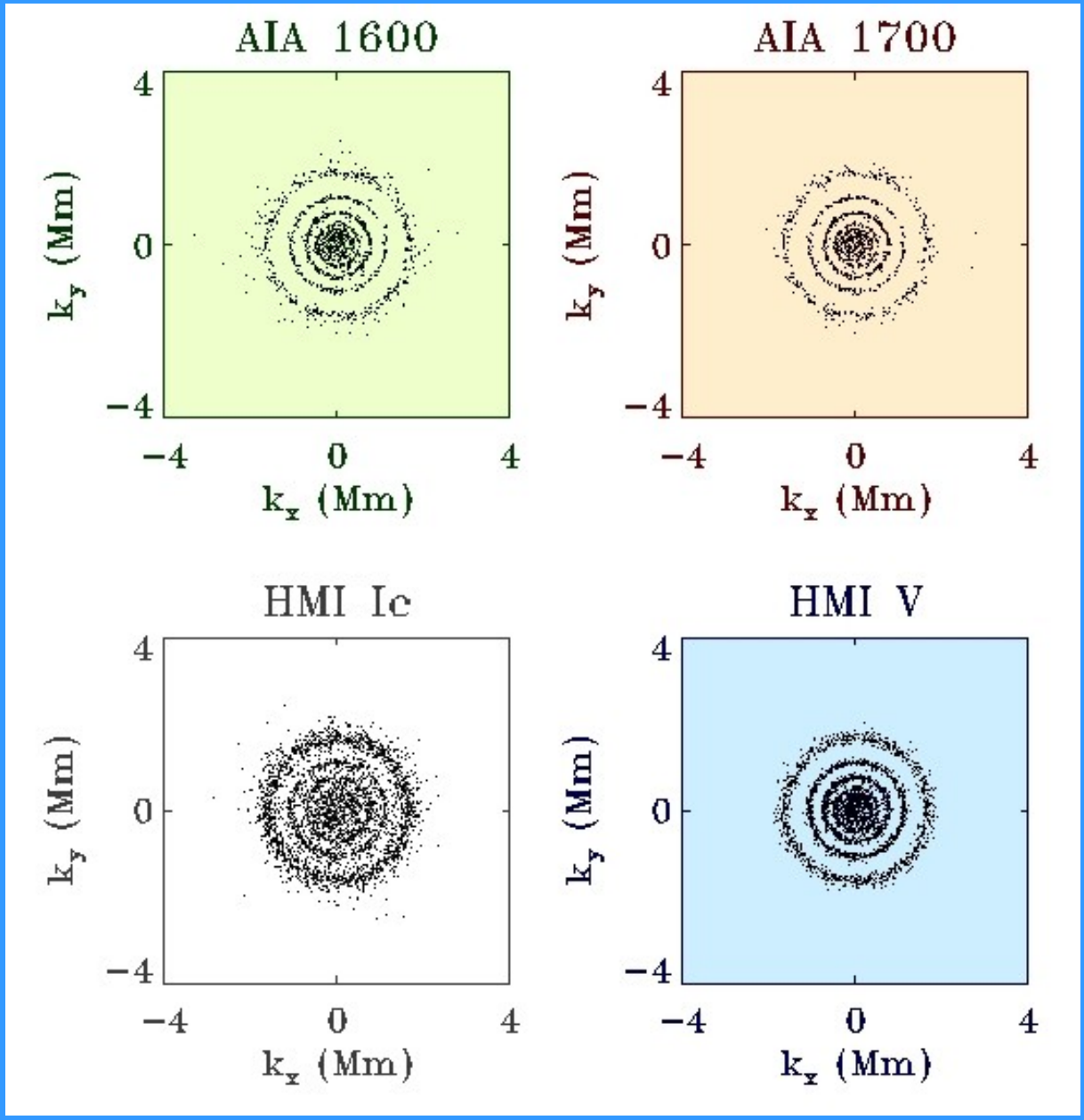

Power Spectra

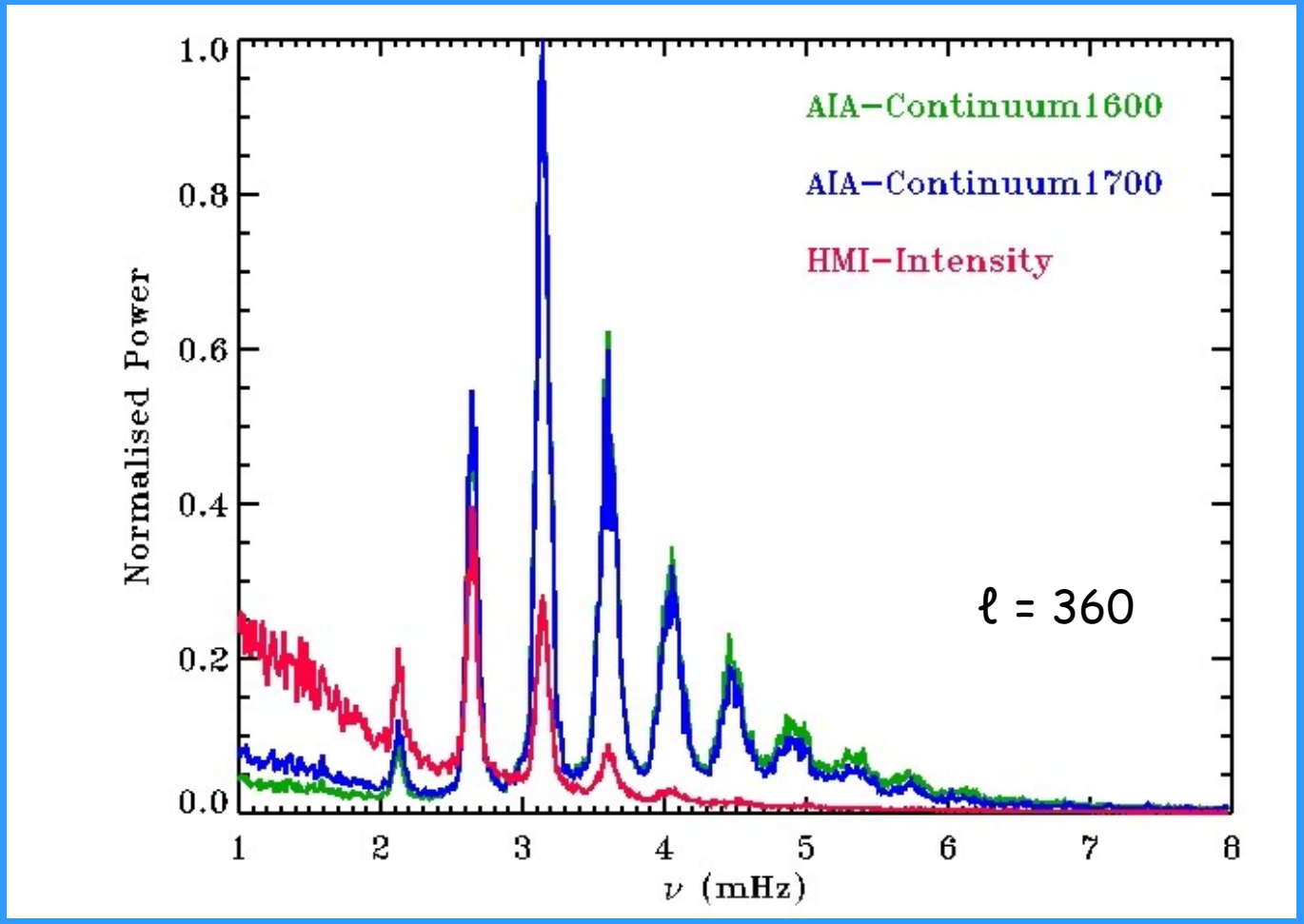

✓Granulation noise in low frequency power spectrum decreases with increasing height of observation.

✓Signal-to-noise ratio also increases with increasing height.

Power Spectra

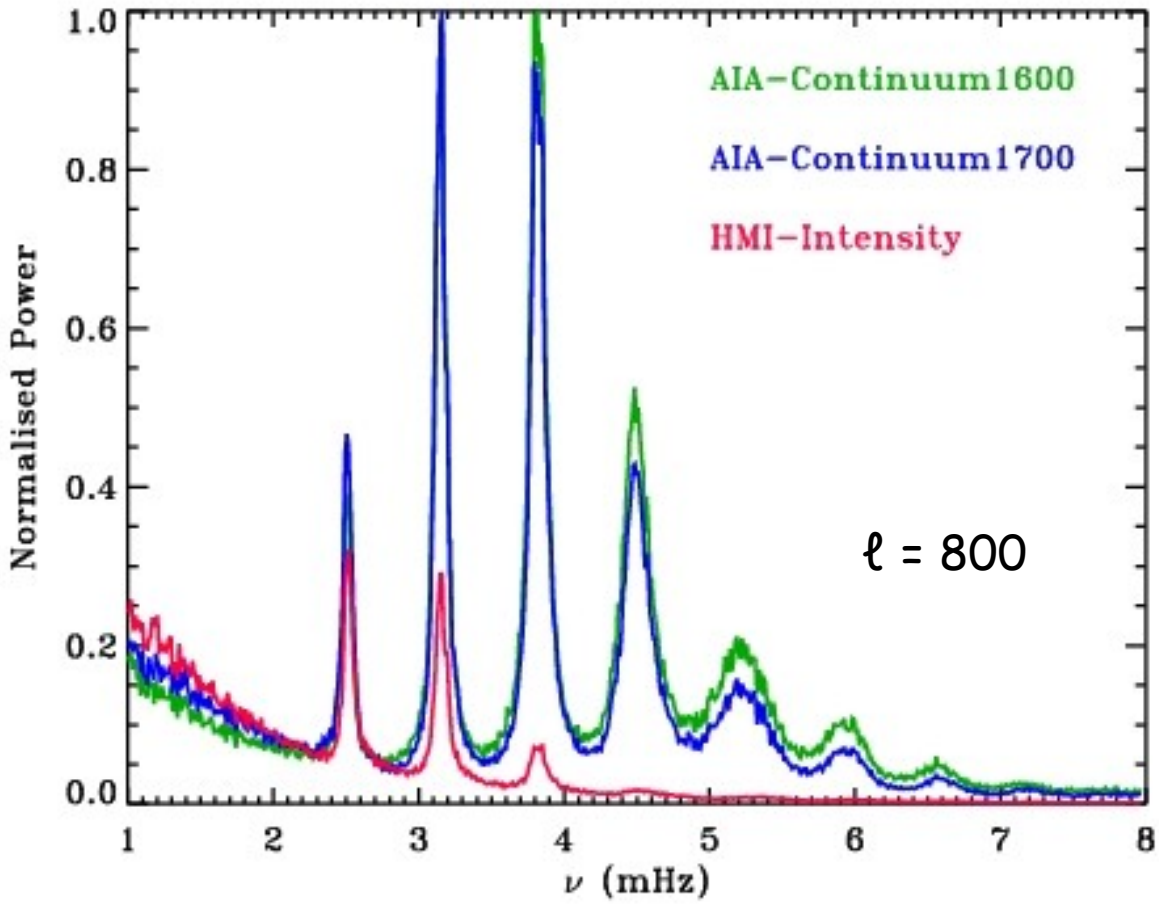

Noise at low frequency frequencies in AIA data also increases at high ℓ.

Asymmetric Fit

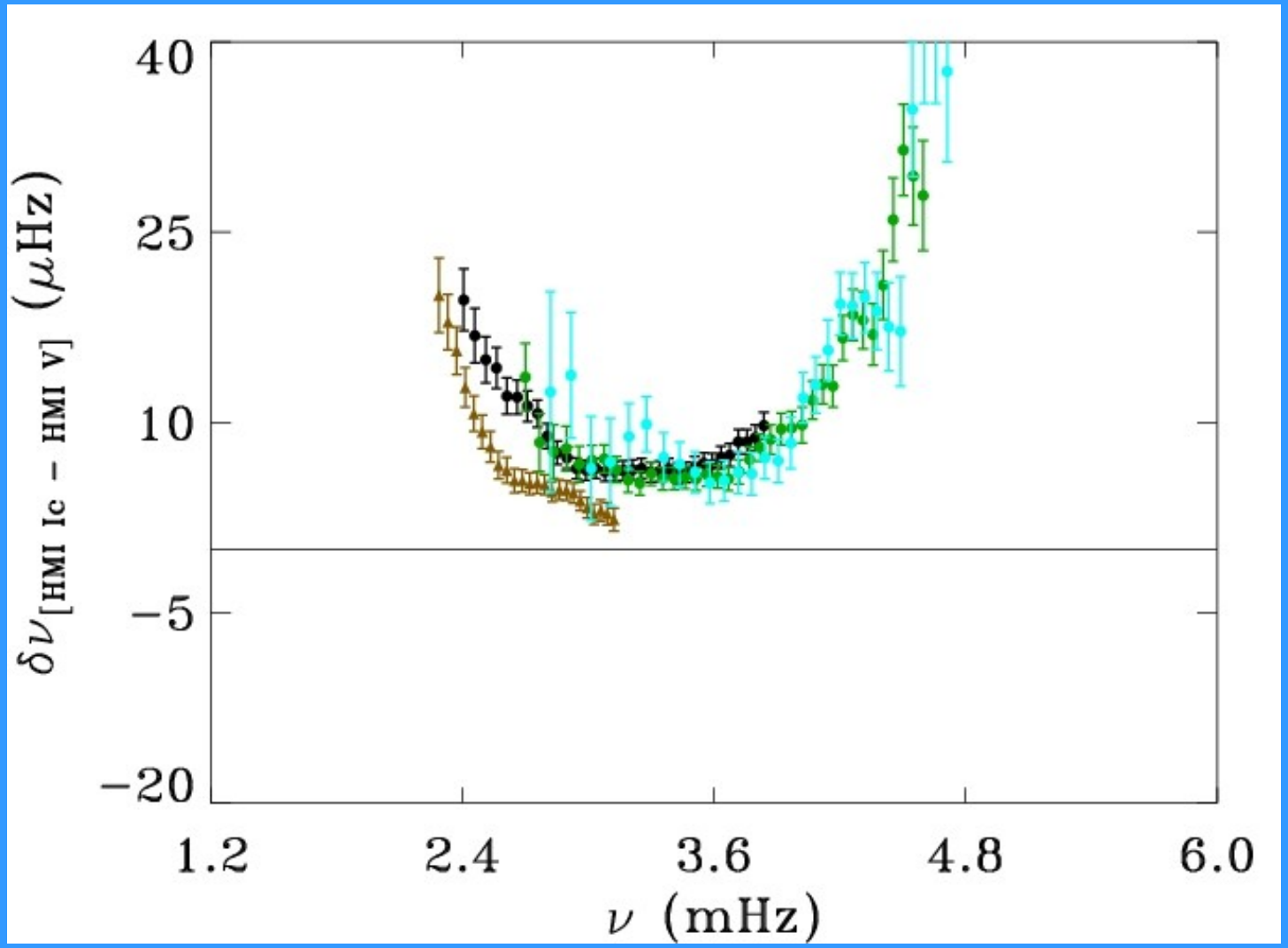

Asymmetric Fit

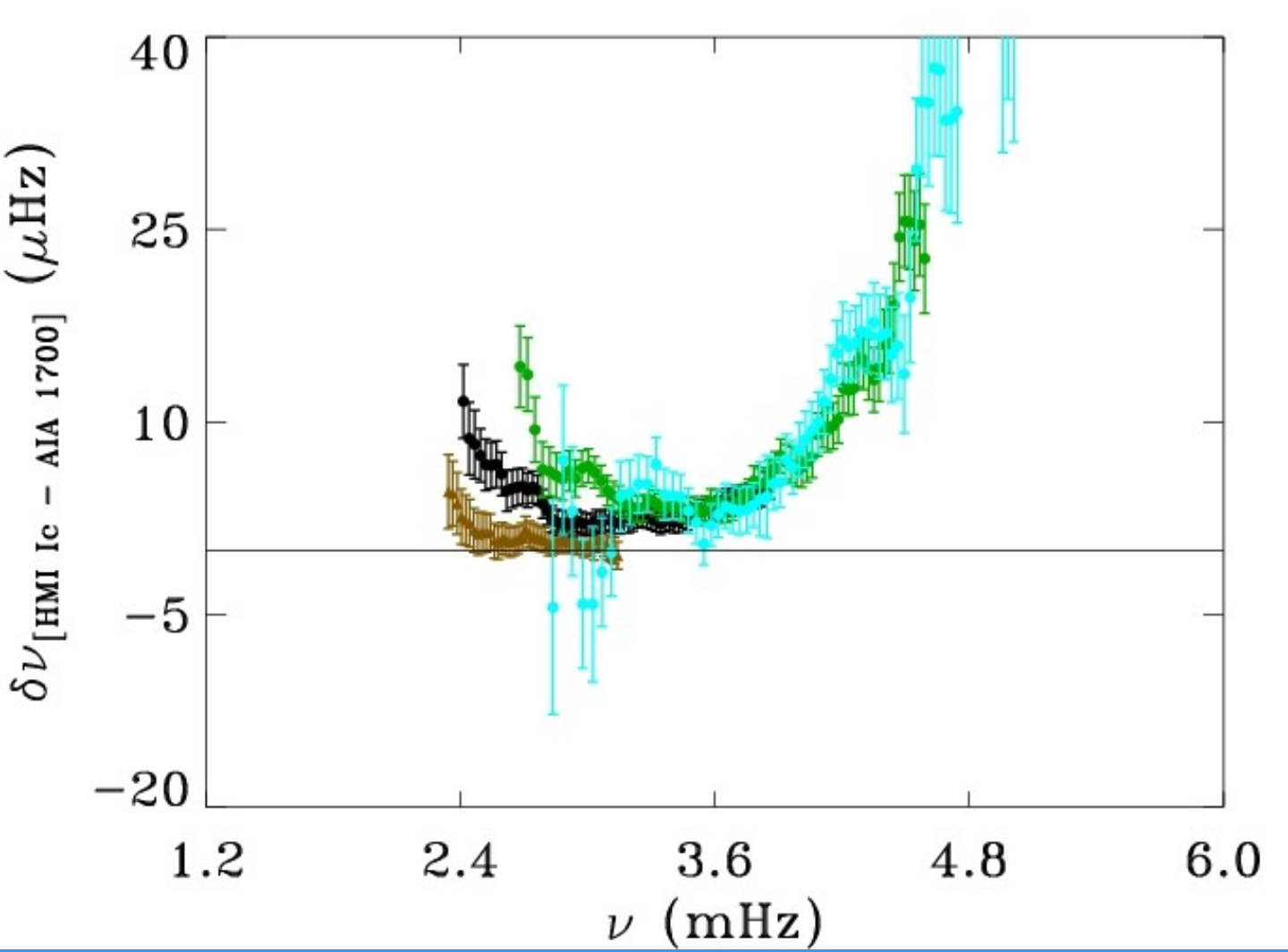

Effect of Systematics on Inferences

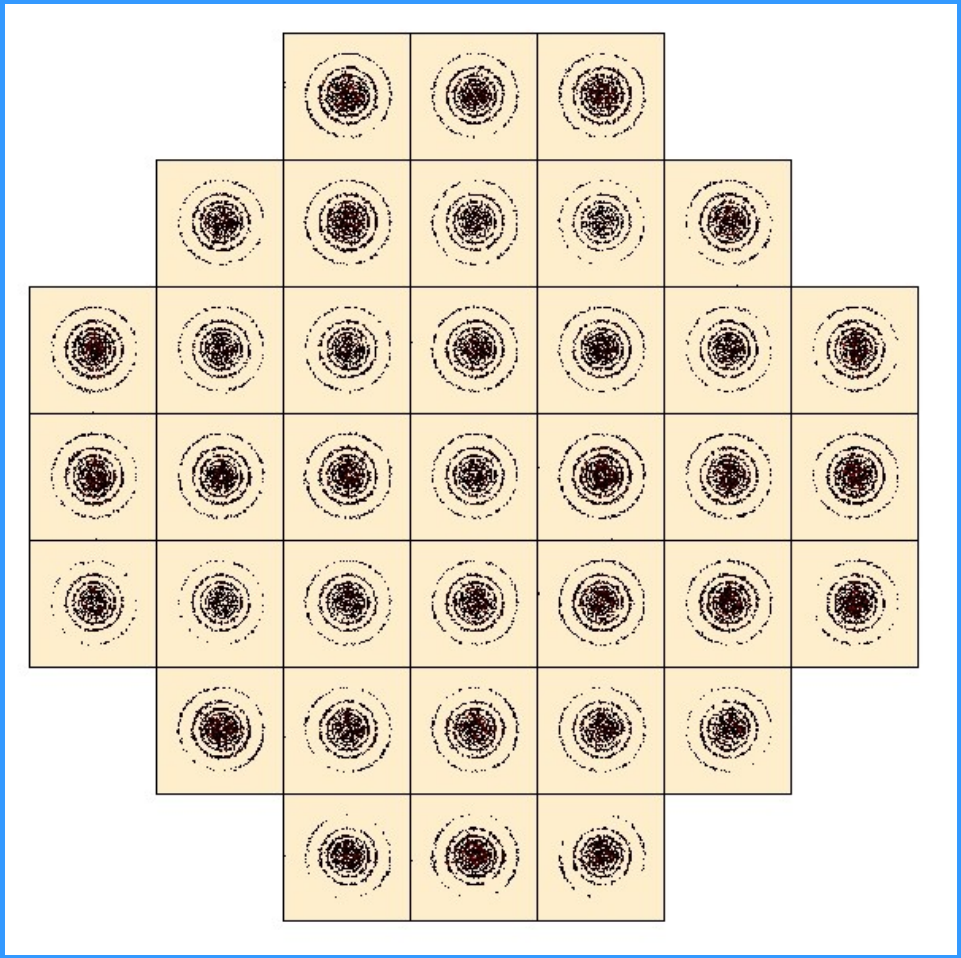

Outlook

- Ring-diagram analysis is a fairly old and mature technique, easy to use and interpret
- HMI is producing massive amount of data in terms of the spatial and temporal resolution and also duty cycle. Thus the technique would also undergo changes
- The difference in sound speed between two different technique is not easy to reconcile and depends on the interpretation. Use of data from simulation and understanding of the effect of magnetic field in the vicinity of active regions would provide further clues.
- Systematic effects e.g. inhomogeneities across the disk needs to be understood and corrected
- The use of subsurface flow parameters have been demonstrated to be useful for the forecasting of space weather
- The 1600 and 1700 Å passbands of AIA have strong 5-minute oscillation signal with low granulation noise and can be used for helioseismic studies.

Thank You